High-Resolution Geophysical Studies of Oceanic Hydrothermal Systems

Maurice A. Tivey and H. Paul Johnson

I. INTRODUCTION

The observation of active hydrothermal vents on the seafloor represents one of the most important discoveries within earth and marine science in recent years. The presence of these vents at mid-ocean ridges provides direct evidence for the existence of hydrothermal circulation within the oceanic crust. The study of this hydrothermal phenomenon is important for a number of reasons that are ultimately related to the processes of oceanic crust formation. For example, the rate of cooling and heat loss of ocean crust can be estimated from temperature and flux measurements of hot-water vents, providing constraints on models of the thermal structure and evolution of the earth. The fluids emanating from the vents can be sampled and their chemistry analyzed to give insight into the source of these fluids, and the geochemical interactions among the fluids, the host rock, and seawater. Geochemical flux measurements and calculations show that hydrothermal vents are an important factor in the global ocean chemistry, representing an estimated 20% of total ocean input for some elements.[1] Hydrothermal vents can form metal-rich sulfide deposits through direct precipitation on the seafloor. This precipitation and the alteration of the host rock are possible analogs for the formation of ancient ore deposits.[2-7] These deposits are of economic and strategic importance as well as of academic interest. The hydrothermal vents also support a self-contained animal community not previously known to exist (see Hessler and Smithey[8] and Desbruyeres and Laubier[9] for reviews). The animal communities cluster around the warm venting water and are supported by the chemosynthesis of sulfur-oxidizing bacteria as an energy source rather than photosynthesis.[10,11]

The original discovery of active hydrothermal vents at mid-ocean ridges came at a time when major technological advances in instrumentation provided the means to study the ocean floor in detail that was never possible before. The development of multibeam echo-sounders (SEABEAM and SASS) have allowed high-resolution, real-time bathymetric maps of the seafloor[12-14] to be made, and together with the use of the global positioning satellite system (GPS) provide a framework within which detailed studies can be carried out. The use of sophisticated side-scan sonar systems such as SeaMARC (seafloor mapping and remote characterization) and GLORIA (geological long-range inclined asdic) generate images of the surface texture of the seafloor, and deep-towed sensor platforms pioneered by the Scripp's DEEPTOW[15] and Woods Hole's ANGUS camera system[16] all combine to give a much higher-resolution picture of the seafloor than has previously been available. This revolution in technology in some sense mirrors an earlier technological revolution when the use of magnetometers and rock-dating techniques led to the Vine-Matthews-Morley seafloor spreading model and a confirmation of plate tectonic theory.

The direction of scientific research also contributed to the search and discovery of active hydrothermal vents at mid-ocean ridges. Within the theory of plate tectonics, scientific hypotheses were maturing on the structure and formation of ocean crust, and the geological processes associated with seafloor spreading. The mid-ocean ridge system was recognized as the locus of new ocean crust formation, which requires at least the ephemeral existence of a magma chamber beneath ridge crests. As new ocean crust forms and moves away from the axis of spreading, it cools and cracks. This process allows seawater to penetrate into the crust and set up hydrothermal convection cells. Through these initial observations it was recognized that, as defined by terrestrial geothermal systems, all the components required for hydrothermal convection were or could be present near mid-ocean ridges.[17] The ocean crust serves as a porous medium for fluid to flow through, a magma chamber furnishes the necessary heat source, and seawater is the fluid for the recharge and subsequent surface discharge system.[17] Accumulating evidence from geophysical measurements of heat flow, the recovery of hydrothermally altered rock samples from dredging and drilling, and geological studies of ophiolites all suggested that hydrothermal convection processes were active within the oceanic crust.

The very nature of hydrothermal vents makes them difficult to locate and study in any detail. Vent systems are commonly located at mid-ocean spreading centers at depths of 2 to 3 km and for the most part cover a relatively small area, on the order of a few hundred square meters. In addition, they are spaced several kilometers apart along the spreading center.[18] Most sea surface mapping techniques have footprints that are larger than individual vent sites, a situation that has encouraged the use of deep-towed equipment to resolve the detail needed. Deep-towed camera systems such as ANGUS[16] provided the necessary groundwork for the location of vent sites and the subsequent use of deep-diving manned submersibles such as

Maurice A. Tivey received a B.Sc. degree in Geology from Dalhousie University, Nova Scotia, Canada, and a M.S. and Ph.D. degree in Geological Oceanography from the University of Washington in Seattle. Dr. Tivey is currently a Postdoctoral Fellow in the Geology and Geophysics Department at the Woods Hole Oceanographic Institution, Woods Hole, Massachusetts. **H. Paul Johnson** received a B. S. degree in Physics from the University of Illinois, Urbana; a M.S. degree in Physics from Southern Illinois University, Carbondale; and a Ph.D. degree in Geophysics from the University of Washington in Seattle. Dr. Johnson is currently a Research Professor in the School of Oceanography at the University of Washington in Seattle.

Reprinted from the CRC Critical Reviews in Aquatic Sciences, Vol. 1, Issue 3, pages 473–496, © 1989 by CRC Press, Inc.

ALVIN, CYANA, and PISCES. Since the initial discovery of active vents on the Galapagos Rift in 1977,[10] other active hydrothermal vent systems have been discovered around the world, from the slow-spreading Mid-Atlantic ridge[19] to the ultra-fast-spreading East Pacific Rise at 20°S[20] (see Figure 1). Evidence for hydrothermal venting has also been observed on off-axis seamounts, abandoned spreading centers (Middle Valley, Juan de Fuca), and fracture zones.[21-23] Geophysical measurements have played a major role in the prediction and discovery of hydrothermal vents, and will continue to play an increasingly important role in the characterization and understanding of the fundamental processes active at hydrothermal vents in the future. First-order questions remain to be answered about the areal and vertical extent of the systems and the spatial frequency of occurrence of the vent systems and their associated deposits. Preliminary measurements of the heat output of vents has been accomplished, but the long-term variations and the relationship of vent output to underlying source mechanisms remain to be addressed. Geophysical measurements are the most useful methods of answering these questions in a quantitative manner. These methods also provide a way to monitor vent systems over various time scales from seconds to years. This review of high-resolution geophysical techniques used to study oceanic hydrothermal vent systems attempts to outline the various methods and results obtained to date and possible future avenues of research and exploration.

II. METHODS

A number of different geophysical techniques can be applied to the search for and characterization of oceanic hydrothermal systems. In this section, the basic physical properties that can be measured are outlined and results from recent geophysical research are reviewed. These geophysical methods can be divided into two basic approaches. The passive method utilizes the natural properties of the earth, such as the gravity or geomagnetic field, microearthquake activity, or the thermal and electrical properties of rocks. In contrast, the active method uses a source to produce a stimulus and then measures the response of the earth to this stimulus. Examples of this method include reflection and refraction seismic profiling, acoustic backscatter information from side-scan sonars such as SeaMARC and GLORIA, and certain electrical methods such as electromagnetics (EM) and resistivity.

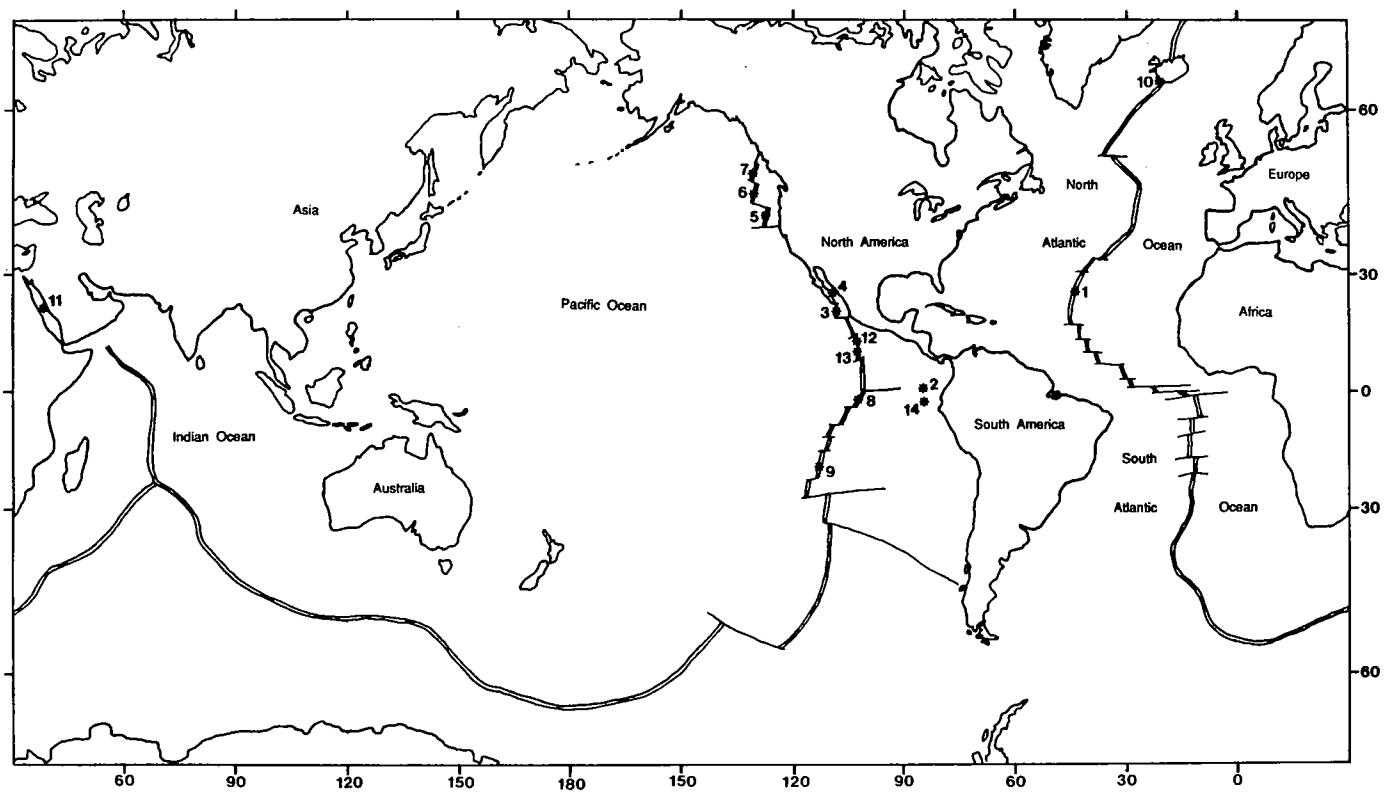

FIGURE 1. World map showing the mid-ocean ridge system and the location of hydrothermal vents discussed in the text. (1) TAG site, Mid-Atlantic ridge, 26°N. (2) Galapagos Rift, 86°W. (3) East Pacific Rise, 21°N. (4) Guaymas basin, Gulf of California. (5) Escanaba Trough, Gorda Ridge. (6) Juan de Fuca Ridge. (7) Explorer Ridge. (8) East Pacific Rise, 3.5°S. (9) East Pacific Rise 20°S. (10) Reykjanes Ridge. (11) Red Sea. (12) East Pacific Rise, 13°N. (13) East Pacific Rise, 11°N. (14) Galapagos Mounds.

In order to study hydrothermal vents, adequate resolution must be provided by the applied technique. Hydrothermal vents are typically located on the seafloor several kilometers below the sea surface, in relatively small clusters, covering an area of about 100 by 100 m.[18,24] Most vent occurrences appear to be preferentially located at the topographic crest of individual ridge segments, which are 30 to 80 km long,[25] although this relationship is not universal.[26] The resolution of sea-surface surveys is generally too coarse to detect the average hydrothermal vent field from the distance of several kilometers. These resolution problems have required the use of deep-towed sensors and deep-diving submersibles for the detailed observation of active vent systems. The extent of coverage of these systems is limited due to low tow speeds of the deep-towed fish and the small observational footprint of the imaging instruments. The use of rapid survey systems and large areal coverage such as SeaMARC and EM may in the future provide new tools to explore and study seafloor hydrothermal vent systems.

A. Thermal Methods

One of the fundamental properties of the earth that is essential to the understanding of many geological processes is the thermal structure of the earth and how it has varied with time. Hydrothermal vents represent a significant mechanism for the loss and transfer of heat from within the earth. Two basic processes for the transfer of heat are appropriate to oceanic systems: conductive heat transfer and convective heat transfer. Conductive heat transfer occurs through a medium due to molecular collision, without mass transfer. The cooling of the oceanic lithosphere has been successfully modeled as a thermal conduction process and can be used to predict the depth of the ocean crust reasonably well.[27,28] Convective heat transfer, on the other hand, is the result of the motion of a medium, such as seawater, through a porous oceanic crust. Hydrothermal vents represent the surface manifestation of convective heat-transport processes that are active within the ocean crust. Hydrothermal vents expel hot water into the surrounding environment, creating temperature anomalies in an otherwise relatively thermally uniform bottom water. This convective type of heat transfer that continues within the overlying water column can be used to locate and map the hydrothermal plumes with deep-towed thermistor chains and other survey vehicles.

Other methods are used to measure the conductive heat transfer or heat flow from the cooling ocean crust. The actual measurement of heat flow involves measuring the thermal gradients within the conductive medium, which in practice is the sediment layer overlying the basaltic basement. Temperature gradients within the sediment column are usually measured by a long probe (2 to 2.5 m long) with thermistor outriggers,[29,30] or by a probe with the "violin-bow" configuration.[31] If heating elements are incorporated into the design, *in situ* conductivity can also be measured. The technique is environment-specific and relies on the presence of sufficient sediment cover to allow for the successful penetration of the sensor. These measurements were originally very time consuming, but recently new sensors have allowed for multiple penetrations and rapid measurements with high accuracy and precision when operated in the "pogo" mode.[32]

It was the use of heat-flow measurements that first suggested the possibility of hydrothermal convection within the ocean crust. Talwani et al.[33] and Lister[34] proposed the existence of hydrothermal convection based on the discrepancy between theoretical values of conductive heat-flow models and the actual measured values near ridge axes. Conductive cooling models of Le Pichon and Langseth,[35] McKenzie and Sclater,[28] and Parker and Oldenburg[27] predict high heat-flow values from near rift axes, but actual measurements show relatively low thermal gradients in these areas.[29,36] Unfortunately, the requirement of the presence of sediments for successful measurements introduces a significant sampling bias, since sediments are not commonly found or are generally not thick enough at spreading centers, where the theoretical heat-flow values predict a maximum. In an attempt to quantify this discrepancy between theoretical and measured gradients, a concerted research effort in the mid-1970s was focused on the Galapagos Rift in the equatorial east Pacific. The equatorial Galapagos Rift at 86°W is one of the few spreading centers where the sedimentation rate is high enough to allow the measurement of heat-flow data close to the spreading rift. The results of early regional surveys showed that thermal gradients were indeed variable and quite low near the spreading center region.[37] Williams et al.,[36] in a detailed heat-flow and deep-towed temperature sensor survey over the Galapagos at 86°W, found a cyclic heat-flow pattern normal to the spreading axis, with a regular variation of high values over faults, bathymetric highs, and sediment mounds. As an added complication, Davis and Lister[38] demonstrated that bathymetry can be important as a focusing mechanism for heat flow, with local topographic highs being areas of high heat flow. From these early results it was suggested that up to 20% of the total heat loss of the earth is through hydrothermal convection, demonstrating the importance of this process in the evolution of the earth as a whole.[36,39] Subsequently, intensive areal heat-flow surveys of the Galapagos Rift[40] and the East Pacific Rise at 21°N[41] have established the existence of regular lineations in the heat-flow pattern parallel to the rift axis. These lineations are suggested to be the result of hydrothermal convection cells within the sediment layer and possibly the upper extrusives. The mean conductive heat flux measured over young crust (0.1 to 1.0 m.y.*) is also found to be one third that of conductive models, i.e., 0.297 W/m^2 (7.1 HFU) measured vs. 0.81 W/m^2 (19.4 HFU) theoretical on the Galapagos Rift[40] and 0.17 W/m^2 measured vs. 0.55 W/m^2 theoretical on the East Pacific Rise.[41] Similar two-dimensional

* Million year.

lineated heat-flow patterns were also mapped by Langseth et al.[42] near the DSDP (deep sea drilling project) hole 504B in 6-m.y.-old crust. Numerical modeling of the Galapagos heat-flow data, based on fluid flow through porous media, can produce a cyclic heat-flow pattern similar to the observed data.[43] The Fehn et al.[43] model predicts that the axial convection cell remains stationary in space, but the off-axis cells move with the lithospheric plate, suggesting the possibility of off-axis hydrothermal convection and areas of continued activity over a long period of time.

There is documented evidence for off-axis hydrothermal activity, most notably in the Mounds area of the Galapagos Rift and more recently in Middle Valley on the northern Juan de Fuca and Guaymas Basin.[23,44] The Galapagos Mounds area is located in a sedimented area 18 to 32 km south of the Galapagos Rift axis at 86°W. The Mounds area is linear and parallel along ridge-strike, and is associated with a zone of relatively high heat flow.[45] The mounds were first noted by Klitgord and Mudie[46] and Williams et al.,[36] and are described in greater detail by Lonsdale.[47] The sediment mounds range in height from 1 to 20 m, with internal temperatures of up to 13°C, and contain significant sulfide mineralization. Approximately 35 heat-flow measurements were carried out by a deep submergence research vehicle (DSRV) —Alvin— in and around the mounds in a detailed survey by Williams et al.[45] The measured thermal gradients were nonlinear and attributed to the movement of interstitial fluids. The observed heat-flow values varied between 0.6 and 32 W/m^2 (15 and 759 HFU, respectively). The general heat-flow pattern, however, is very complicated, and the study of these hydrothermal mounds still requires major work.

Middle Valley is a sedimented spreading center on the northern Juan de Fuca Ridge where spreading has recently ceased, but there are a number of currently venting hydrothermal mounds within the valley. Davis et al.[23] have completed a detailed heat-flow survey in and around the actively venting mounds. Their results show measured heat-flow values of 2.9 W/m^2 over an active mound relative to a background heat flow of 0.4 W/m^2. Other sedimented sites could benefit from such a detailed survey, such as in the Escanaba Trough on the Gorda Rise.[48]

In contrast to conductive methods, convective measurements involve the direct measurement of the thermal properties of seawater. Temperature sensors such as thermistors and thermocouples can measure the amplitude and gradients of seawater temperature anomalies. These thermistor arrays are usually towed through the water column a few hundred meters above the seafloor. Care must be exercised, however, in the interpretation of temperature data without any pressure (depth) corrections, since the observed anomalies could be due to adiabatic mixing effects. An effective measurement technique has been the use of a CTD (conductivity, temperature, and depth) sensor so that the mixing effect can be removed. Recently, near-bottom deep-towed sensors have been used to conduct reconnaissance-style surveys measuring the three-dimensional structure of plumes[49] and the variation of hydrothermal activity along the strike of a spreading center.[19,50] Water temperatures have also been measured directly at the source, i.e., at chimney exits, to determine source characteristics and individual vent heat output.

Although heat-flow measurements suggested the presence of hydrothermal activity, it was the measurement of water temperature anomalies (i.e., convective heat transfer) that provided the first direct evidence. Spike-like temperature anomalies measured over the Galapagos Rift at 86°W by the deep-tow thermistor chain of Williams et al.[36] provided incentive for closer examination. Weiss et al.,[51] on the basis of the above "Williams spike", was able to delineate a water temperature anomaly with CTD work and actually sample fluid from the region of the temperature anomalies over the Galapagos. Analysis of the samples revealed excess quantities of helium-3 and radon, indicating that these fluids are mantle-derived, providing the first incontrovertible evidence of hydrothermally circulating seawater at a spreading center.[51,52] Detrick et al.,[53] in another deep-tow temperature survey over the same Galapagos region, found no thermal anomalies that could be attributed to vents, showing that convective water temperature anomalies can be intermittent.

In the Atlantic Ocean, evidence for hydrothermal activity was suggested by the dredging of hydrothermally altered rocks[54,55] and the measurement of a 0.11°C thermal anomaly in a 1974 thermistor survey over the Trans-Atlantic geotraverse (TAG) area of the Mid-Atlantic Ridge.[56,57] The possibility of oceanographic effects as the source of thermal anomalies could not be ruled out, however, due to the lack of coincident salinity data (see Fyfe and Lonsdale[22] and Fehn et al.[58] for arguments against using temperature data alone as indicators of venting anomalies). A deep-water temperature survey over the FAMOUS (French-American Mid-Ocean Undersea Study) area on the Mid-Atlantic Ridge failed to find any unambiguous hydrothermal temperature anomalies.[58] Near-bottom water temperature measurements on the East Pacific Rise at 21°N, using the Scripps DEEPTOW with a quartz crystal temperature probe, found thermal anomalies of 0.04 to 0.07°C located over the axis of spreading.[59] From these data, Crane and Normark[59] concluded that hydrothermal venting was taking place from ridge-parallel zones of fissuring on each side of the main extrusive zone. Heat-flux calculations based on a simple line-source model produced an average heat flux of 7.1 W/m^2 for the central 6-km width of the spreading center. Subsequent submersible dives to the south of this area found massive sulfides[3] and active black and white smoker hydrothermal vents.[2] In a survey over the sedimented axial rift of the Gulf of California (Guaymas Basin), the Scripp's DEEPTOW CTD measured 20 thermal plumes at heights of 10 to 100 m above the seafloor.[44] This region of temperature anomalies was later visited by a submersible, which found low-temperature venting

(<100°C), and occasional high-velocity (2 m/s) high-temperature (270 to 314°C) chimneys.[44]

On a more regional scale, Crane et al.[50] carried out a SEABEAM, deep-towed SeaMARC I, and near-bottom thermistor survey along the axial portion of the Juan de Fuca Ridge. The survey delineated five separate hydrothermal vent fields on individual ridge segments spaced approximately 100 km apart: the southern symmetrical segment (SSS), the axial seamount, the northern symmetrical segment (NSS), the Cobb propagator tip (Surveyor volcano), and the Endeavour segment (see Figure 2). The heat flux generated by the mapped vent sites was calculated using two different models based on the observed temperature anomalies (see Table 1). A simple line-source model gives heat-flux values of 172 to 7337 MW for the individual sites, or a total value of 13,000 MW for the entire ridge (141 km) (see Table 1). In the second model, as the water column moves across the ridge axis at some velocity, it is heated by the vent fields. There were no measurements of the mean flow rate across the ridge at the time of this survey, but for a mean flow of 1 cm/s the heat flux ranges between 3000 and 80,000 MW for the individual vents, totaling 150,000 MW for the entire ridge (see Table 1).[50] A more detailed survey over the SSS by Crane et al.[50] showed that the heat flux was concentrated in only two areas. Point-source models give heat-flux values of 1.6 MW, whereas line-source models give heat-flux values of 814 MW (see Table 1 for comparisons with other values). This analysis shows the large uncertainties in this method of mapping the heat flux from hydrothermal vents. A more comprehensive survey of the Endeavour and SSS vent areas is described by Baker and Massoth,[49] using the deep-towed temperature, salinity, and transmissometer instrument named SLEUTH. Their measurements have significantly improved the estimation of heat flux from vent fields by mapping the three-dimensional nature of vent plumes over hydrothermal areas. The SLEUTH vehicle is towed at 2 to 3 km/h and depth-cycled in a sawtoothed fashion to delineate the top and bottom of the plume layer, which is monitored by real-time data telemetry. Heat-flux calculations by Baker and Massoth,[49] using a method similar to model 2 of Crane et al.,[50] produced a net heat flux of 1700 ± 1100 MW from the Endeavour vent site, and 580 ± 351 MW from the SSS site. These values are much lower than the initial model 2 estimates by Crane et al.[50] (see Table 1) for the Endeavour and SSS sites. For the Baker and Massoth[49] survey, the mean current flow in the Endeavour area was independently measured by static instrumented moorings.[60] These results demonstrate that a knowledge of the three-dimensional nature of the vent plumes is essential in calculating reliable heat fluxes.

In a reconnaissance survey over the southern Juan de Fuca Ridge, the SLEUTH device discovered a large plume 700 m thick and 20 km in diameter over the southern Juan de Fuca in 1986.[61] This plume, named "Megaplume", contained particles that could settle at rates of 200 m/d, but was distinctly

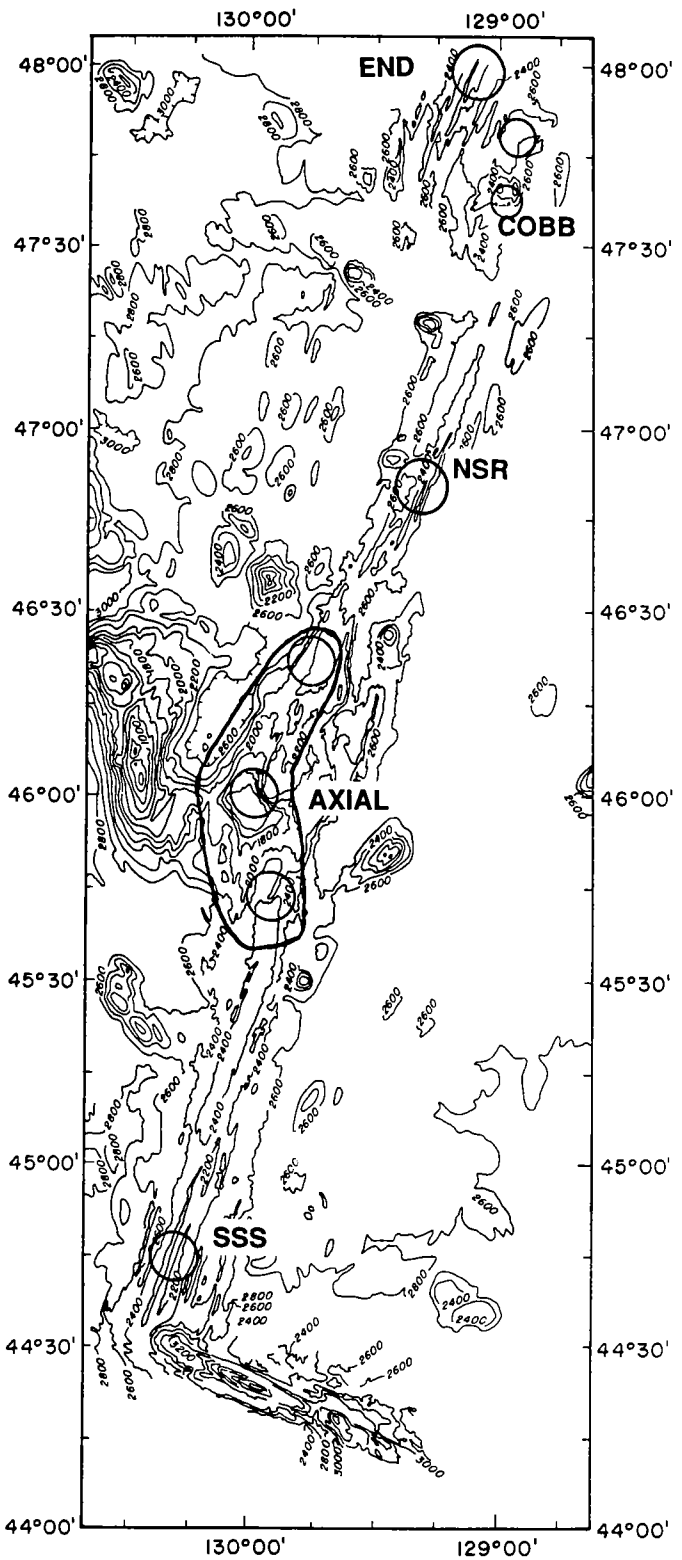

FIGURE 2. Seabeam bathymetry of Juan de Fuca Ridge, showing the location of hydrothermal fields mapped by Crane et al.[50] in 1982. (SSS = southern symmetrical segment; AXIAL = Axial seamount; NSR = northern symmetrical Ridge; COBB = Cobb overlapper or Surveyor Seamount; END = Endeavour Ridge.)

Table 1
Comparison of Calculated Heat-Flux Values from the Juan de Fuca Ridge

	Calculated heat flux (MW)				
Vent field	1	2	3	4	5
SSR	2,096	30,240	1.6	814	580 ± 351
Axial	7,337	81,890			
NSR	2,266	28,220			
Surveyor smt	172	3,020			
Endeavour	1,133	12,600			1700 ± 1100
Total	13,004	155,970			

Note: SSR = Southern symmetrical ridge, NSR = northern symmetrical ridge.

1. Crane et al.[50] Model 1 line source.
2. Crane et al.[50] Model 2 flow model at a velocity of 1 cm/s.
3. Crane et al.[50] Detailed survey, point-source model.
4. Crane et al.[50] Detailed survey, line-source model.
5. Baker and Massoth,[49] 3D survey flow model type.

separate from the steady-state, near-bottom plume of the active hydrothermal vents in this area. Surveys in the same region 3 months later showed that Megaplume had vanished, supporting the hypothesis that it was the result of a cataclysmic type of event.[61] The heat energy contained in Megaplume (6.7×10^{16} J) was equivalent to the annual output of 200 to 2000 high-temperature vents. The source of the plume is not known, but speculations include some volcanic or crustal fissuring event, with possible extrusion of lava flows and the resultant heating of the surrounding seawater.[61] The observation of Megaplume points out the importance of episodic events on the heat and chemical inputs into the oceanic system, and a fundamental lack of data on these kind of events.

To avoid oceanographic mixing effects and all the other necessary assumptions made in plume studies, a number of experiments have focused on measuring the heat flux directly at the vent orifices and then extrapolating up into the plume environment in the water column. The essential measurements usually involve the temperature and velocity of the venting fluids. The first such measurements were made at the Galapagos vent field, where fluid exit temperatures of approximately 17°C and flow rates from 0.02 to 0.1 m/s were estimated.[10] The warm venting fluid rose in plumes to almost 180 m above the seafloor before dispersing horizontally. At the East Pacific Rise vent site at 21°N, flow rates of 1 to 5 m/s and vent orifice diameters of 4 to 40 cm were estimated from video tape and film of black smoker vents to give a heat-flux value of 250 MW (for the National Geographic Vent).[62] In an effort to obtain more quantitative measurements of hydrothermal vent heat flux, Converse et al.[63] directly measured flow rates and temperatures of smokers at the 21°N East Pacific Rise vent site using a small vane-type flowmeter. The particulate effluent impaired the operation of the flowmeter after only a few seconds, but useful data were recorded. The measured exit temperatures ranged between 275 and 350°C at flow rates of 0.7 to 2.4 m/s. Using buoyant-plume theory, the heat flux of individual vents was calculated to be between 0.5 and 10 MW (National Geographic Vent), with the total heat flux for all three vents (National Geographic, OBS, and Southwest vents) estimated to be approximately 220 ± 80 MW. The heat flux from the warm vent sites was not measured, but was estimated to be on the order of 12 to 900 MW for 0.1 m/s flow rates of 20°C fluid.[63]

To characterize the intermediate scale (i.e., between the detail of the Converse et al.[63] and Macdonald et al.[62] experiments and the kilometer scale of the Crane et al.[50] and Baker and Massoth[49] surveys), simultaneous velocity, temperature, and conductivity measurements were made over a small vent field at 11°N on the East Pacific Rise.[24] A submersible with a 50-m, vertically extended instrument cable was used to map the convective flow above the vent field. Exit temperatures were measured at 338°C with flow rates of about 0.1 to 0.2 m/s at 24 m above the vents or 0.6 m/s at vent exit ports. A buoyant-plume model gives a calculated heat flux estimate of 3.7 ± 0.8 MW. This estimate is of the same order of magnitude as the calculations of individual vent heat fluxes by Converse et al.[63] over the East Pacific Rise at 21°N. Using the same simple plume approximation as Little et al.,[24] the calculation of heat flux from one vent at the Endeavour ridge site gives 2.5 MW (unpublished data), which is within the range of the above calculations.

Thermal methods from the beginning have been important in the prediction and confirmation of the presence of hydrothermal convection processes within the ocean crust. The conductive heat-flow data have demonstrated that the low heat flow at spreading centers is a result of convective heat losses, with as much as 30% of the available heat flux from the lithosphere being removed by convective heat transfer.[34,36,64] Fine-scale heat flow near ridge crests has been shown to be spatially cyclic on the scale of a few kilometers and indicates the strong possibility of off-axis convection. The implications for the alteration history of crustal rocks and its physical properties are enormous. If off-axis convection cells remain active and move with the plate, then significant crustal alteration will result, producing a laterally inhomogeneous crust, with the ensuing consequences of such a situation. If, on the other hand, convection cells remain fixed with respect to the ridge axis, then the crust may be uniformly altered as it moves through different zones.[65,66]

Detailed vent studies have produced accurate quantitative estimates of the heat output of individual smokers (0.5 to 10 MW); however, estimates of diffuse warm-water venting remain vague and qualitative, but are not likely to be improved upon in the near future. Perhaps the best method yet used to characterize a vent system is by doing water column plume

studies, where the heat and mass fluxes from entire vent systems are mapped. Deep-tow devices of the SLEUTH design have shown the most promise in mapping the three-dimensional nature of the effluent plumes over hydrothermal vents. The plume surveys evaluate the integrated heat flux from a vent site, including the hot smokers and background warm diffuse flow. The steady-state vs. episodic controversy of the venting fluid remains unresolved, and certainly the temporal variations of vent output could be effectively measured by the plume approach. The fortuitous measurement of the Megaplume anomaly dramatically demonstrates the importance of the episodic nature of seafloor processes, as well as the need for denser time-series measurements. The establishment of long-term observations of the seafloor would go a long way toward resolving these questions.

B. Magnetics

The measurement of magnetic anomalies is both rapid and efficient, and involves measuring the variations in the ambient magnetic field of the earth, and removing the theoretical dipole field of the earth or International Geomagnetic Reference Field (IGRF) to give the resultant magnetic anomaly field. The interpretation of magnetic anomalies is generally more complex than that of gravity anomalies, due to the dipolar nature of the geomagnetic field compared to the polar gravity field. Magnetic anomalies arise from the contrasts of magnetic properties of minerals in the underlying rocks or from variations in the direction of magnetization (i.e., reversely magnetized vs. normally magnetized). Titanomagnetite is the main magnetic mineral responsible for the magnetism of oceanic crustal rocks, but there are other magnetic minerals that can be locally important, such as pyrrhotite and hematite.

Magnetics have played a key role in the realm of plate tectonics since the beginning of modern plate tectonics in the early 1960s. It was the discovery and interpretation of linear magnetic anomalies over ocean crust that led to the development of the seafloor spreading hypothesis.[67] The Vine-Matthews hypothesis was one of the breakthrough discoveries in the development of plate tectonics. That hypothesis proposed that the reversals in the magnetic field of the earth are recorded by the upper basaltic ocean crust as it forms and moves away from a mid-ocean ridge, resulting in the observed linear marine magnetic anomalies (or "magnetic stripes"). The source layer responsible for the marine magnetic anomalies has been the subject of intense debate for many years (see Harrison,[68] Banerjee,[69] and Johnson[70] for reviews), but there is general agreement that the upper ocean crust contributes the major portion of the observed magnetic signal.

The process of hydrothermal circulation within the ocean crust has a major impact on the chemistry and petrology of the host rock. An integral part of this basalt-seawater interaction is the response of the magnetic minerals to the changes that occur. The primary magnetic mineral in oceanic basalts is titanomagnetite, an iron titanium spinel with a characteristic composition of 62% ulvospinel.[70,71] The ferrous ions in titanomagnetite are very sensitive to alteration, and these changes are reflected in the magnetic properties of the mineral and its alteration products. There are a number of studies of the alteration of basalt by seawater using natural samples obtained by dredge programs, deep drill holes, and laboratory experiments (see Honnerez,[72] Thompson,[73] and Mottl[74] for reviews). The alteration of basalt is generally classified according to temperature and can be divided into three types. Low-temperature alteration, or "submarine weathering", occurs at ambient seafloor temperatures or below some arbitrary temperature (e.g., <50°C) at which the first truly metamorphic minerals occur.[66,72] Hydrothermal alteration occurs at elevated temperatures, but usually below 500°C, and results in the formation of greenstones in the zeolite, greenschist, or amphibolite facies grade of metamorphism. High-temperature alteration or "deuteric" alteration occurs at temperatures above 600°C, usually during the initial cooling of the rock, but is not commonly seen in submarine basalts.[79] The magnetic properties of the basalts show characteristic variations depending on both the type of alteration and the temperature at which it occurred.

Low-temperature alteration has been studied in great detail (see Honnerez[72] for a review) and the effect upon the magnetic properties has been well documented.[75-78] The low-temperature alteration of basalts is characterized by the oxidation of highly magnetic titanomagnetite to less magnetic titanomaghemite and the eventual conversion to nonmagnetic sphene. With increasing alteration, the initially low curie temperatures (<160°C) increase along with magnetic stability, while magnetization intensity decreases by almost a factor of ten. These effects are demonstrated by the overall decrease in sea-surface magnetic anomaly amplitudes with increasing crustal age, and the parallel decrease in magnetic intensity of basalts with distance from the spreading center.[75,76,78]

The hydrothermal alteration of basalts has also been studied in some detail,[66,74,79] but the effect upon the magnetic properties is not as well understood as that of low-temperature alteration.[80-83] Temperatures up to 200 to 250°C may simply expedite the oxidation process of low-temperature alteration, but different effects occur at higher temperatures. The titanomagnetite suffers "phase-splitting", in which a titanium-rich phase separates from the titanomagnetite and forms ilmenite exsolution lamellae within the magnetite. At hydrothermal temperatures, this exsolution is usually submicroscopic.[83] Several steps in the hydrothermal alteration of titanomagnetite have been outlined, progressively from granulation (the submicroscopic exsolution of ilmenite from the primary titanomagnetite) to the replacement of ilmenite by sphene, and, finally, the eventual, complete replacement of the magnetite grains by anatase and the formation of secondary magnetite.[82] As far as the rock magnetic parameters are concerned, curie temperature and magnetic stability increase during this process. Initial hydro-

thermal alteration may increase the magnetization slightly due to the ilmenite-magnetite phase separation, but as alteration becomes pervasive, magnetization intensity decreases as the magnetite is replaced by nonmagnetic silicates.[81-83]

High-temperature alteration of igneous rocks (both oceanic and continental) results in the early phase splitting of titanomagnetite into magnetite and ilmenite. The curie temperatures, stability, and magnetization all increase due to the high-temperature alteration, but this is rarely seen in ocean extrusive basalts, although it appears common in the sheeted dike complex.[71]

On the larger scale, the style and extent of the ocean crust alteration will be influenced by the existence and morphology of the hydrothermal convection cell geometry. High temperatures in upflow zones will result in extensive and rapid alteration, while downflow zones will encourage low-temperature alteration of the host rock. If convection cells are fixed with respect to the ridge,[43] then the crust will pass through different upflow/downflow zones with age and be uniformly altered laterally, with possible small-scale fluctuations. If convection cells are fixed with respect to the accreting plate,[65] then a laterally inhomogeneously altered crust would result. These large-scale variations in crustal alteration could result in changes in the magnetic properties of the source layer, which may account for the fine-scale magnetic anomaly variations that are observed.[83] The existence of magnetic anomalies that are due solely to variations in hydrothermal processes rather than geomagnetic field reversals are thus a real possibility.

The presence of a characteristic magnetic signature over a hydrothermal area has been supported by a growing body of observational evidence. Magnetic anomaly lows have been found that were associated with terrestrial hydrothermal areas such as the Wairakei geothermal area in New Zealand,[84] where magnetite in the underlying crustal rocks has been converted to pyrite through hydrothermal alteration, and in Rabaul, New Britain[85] and the Salton Sea.[86,87] In a magnetics survey over Lake Kinneret, Israel, positive magnetic anomalies were found that were associated with hot springs that were depositing magnetite.[88] Closer analogs to oceanic hydrothermal systems are found in ancient ophiolitic deposits such as the Troodos ophiolite in Cyprus. Johnson et al.[89] reported that a low-level magnetic survey over a massive sulfide ore body in the Troodos ophiolite showed a pronounced magnetic anomaly low associated with hydrothermal alteration of the host basaltic rock. An even closer analog to oceanic hydrothermal systems is the Reykjanes hydrothermal field in Iceland on the axis of the Mid-Atlantic Ridge, which exhibits a regional magnetic low of approximately 200 nT.[90]

A number of marine magnetic investigations have demonstrated the presence of magnetic anomaly lows in the vicinity of hydrothermal systems. In the Red Sea, a magnetic field low (650 nT) was discovered over the Atlantis II deep, which has a 100°C active brine pool. The adjacent Chain and Discovery deeps, which have no brine pools, show no similar anomaly lows.[91] The sgnificance of this low was not noted at the time.[91-93] Macgregor and Rona[94] and Macgregor et al.[95] suggested that an observed sea-surface magnetic anomaly low of 200 nT over the TAG area of the Mid-Atlantic Ridge was due to hydrothermal alteration of the basaltic crust. The anomaly covered a region of 5 km, suggesting a significant area of alteration, if indeed the source of the anomaly low was hydrothermal alteration. Recent discoveries of actively venting sites within the same area have subsequently confirmed the magnetics data evidence.[19]

One of the problems of identifying magnetic anomaly lows at the sea surface due to hydrothermal activity on the seafloor is the attenuation of the magnetic signal with distance from the source. Sea-surface magnetic anomalies have been filtered by the distance from the source, i.e., the seafloor, resulting in a maximum resolution of only 3 to 4 km.[96] In an effort to study the local magnetic field over a hydrothermal field, Tivey and Johnson[97] completed a near-bottom magnetics survey over hydrothermal vents on the Endeavour segment of the Juan de Fuca Ridge. This survey (see Figure 3) showed that there was a magnetic anomaly low (300 nT) over one vent site and a magnetic anomaly high (600 nT) over an adjacent vent site only 100 m away. Figure 3B shows the temperature anomalies measured at the same time as the magnetic field, indicating the location of active vents. There appeared to be no obvious difference in the surface geology or mineral composition between the two sites.[6,98] A number of recovered sulfide samples contain high concentrations of pyrrhotite, which possesses a high remanent magnetization. The magnetic anomaly high may represent an overall greater concentration of pyrrhotite in one vent size compared with the other, or alternately, the possible presence of a magnetic (magnetite) body at depth.

In a separate survey, a deep-tow magnetics profile across the Endeavour Ridge in the area of the vents showed that the central anomaly magnetic high as seen at the sea surface is in fact a double-peaked anomaly near the seafloor with an anomaly low over the rift valley.[99] This anomaly low may represent the effect of hydrothermal demagnetization within the rift valley. An alternate possibility, based on an axial low over the East Pacific Rise at 20°S, is that the curie isotherm is close to the surface beneath the rift valley due to a shallow magma chamber, thus reducing the thickness of the magnetic source layer.[100] A similar near-bottom magnetics survey over an extinct hydrothermal stockwork zone site on the Galapagos at 86°W[101] showed no measurable anomalies associated with the extinct sulfide sites, but instead showed a large-scale general anomaly low over the southern valley floor due to regional hydrothermal alteration of the entire area. The lack of any associated anomaly over the sulfide deposits is probably due to the higher copper content and the absence of pyrrhotite.

In summary, the magnetic properties of ocean crust can be affected by hydrothermal convection processes. Depending on

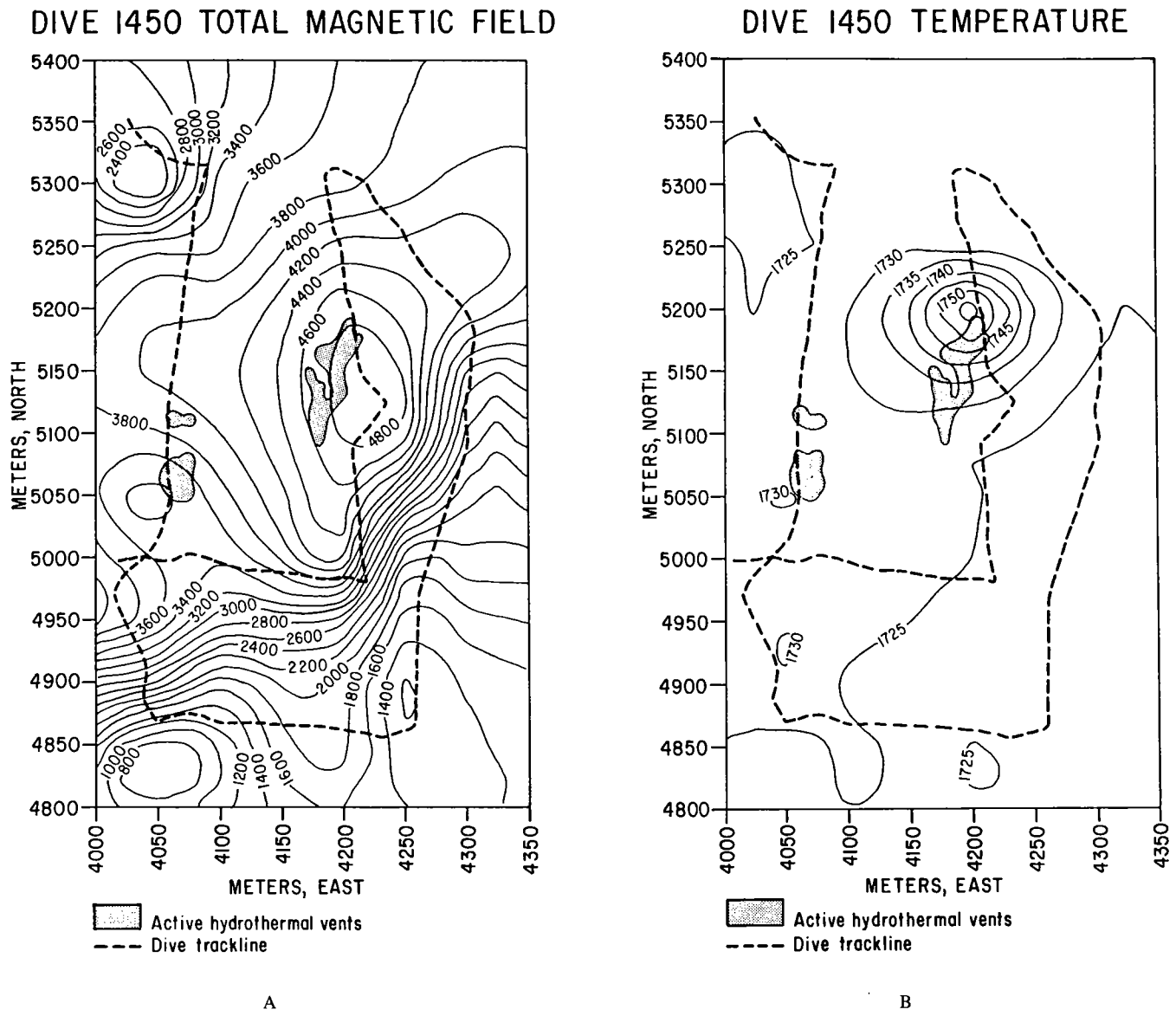

FIGURE 3. (A) Near-bottom total magnetic field anomaly over the Endeavour hydrothermal site, Juan de Fuca Ridge, measured on a level plane 50 m above the seafloor. The contour interval is 100 nT. (B) Temperature anomalies locating individual vents at the Endeavour hydrothermal site, Juan de Fuca Ridge, at an altitude of 50 m above the seafloor. The contour interval is 5 m°.

the style and geometry of the convection cells, the ocean crust alteration state may be laterally inhomogeneous, which could give rise to fine-scale magnetic anomaly variations. It is unlikely that sea-surface magnetics will show any variation over individual vent sites, but may show the kilometer-scale variations due to regional convective and alteration processes. Detailed magnetic surveys over vent sites can provide clues to the composition, structure, thickness, and extent of sulfide deposits, but the technique is inherently nonunique, and other methods are required to validate any conclusions drawn from magnetic work.

C. Electrical Methods

Electrical geophysical methods encompass a wide range of approaches, including self-potential (SP), induced potential, resistivity, telluric currents and magnetotelluric fields, electromagnetics (EM), audio frequency magnetics, and more. The underlying principle of these techniques makes use of the electrical properties of the underlying rocks and the effects of currents flowing within the rocks. Electrical properties of oceanic rocks are affected by a number of effects, including electrical potentials and current, the electromagnetic fields created by the naturally flowing currents, and artificially induced current

effects. The different electrical methods can be classified into two basic categories based on the use of natural sources, the "passive method", or the use of induced or artificial sources, the "active method".

Electrical methods have been widely used on land for many years in the exploration of sulfide-rich ore bodies[102,103] and in the oil industry as a downhole logging tool. Spontaneous potential (also known as self-potential), or SP, is an example of the passive method that measures the electrical potentials that build up in the ground as a result of thermal and chemical gradients and the flow of fluid within the rocks. In 1960, Sato and Mooney[104] published a landmark paper on the theory of SP, which proposed an oxidation-reduction mechanism for the generation of current flow within an ore body and the electrical potential field around the body. Sulfide ore bodies usually produce negative SP anomalies in relation to the surrounding rock with typical anomalies ranging from a few millivolts to 1 V.[105] SP is one of the simplest quantities to measure, requiring only a pair of electrodes and the ability to measure the potential difference between them.

Electrical resistivity of crustal rocks, as an example of the active exploration method, can be measured between the electrodes by passing a current through them and measuring the potential difference across them. From these measurements an apparent resistivity can be calculated, and through an empirical relationship (Archie's law), the porosity of the crustal units can be calculated.[106,107] A profile of electrical resistivity with depth can provide estimates of a number of different parameters, such as bulk density, porosity, water content, and compressional wave velocity.[108] The presence of conductive groundwater in many terrestrial hydrothermal systems has been successfully mapped with resistivity and electrode arrays.[109]

The discovery of polymetallic sulfide deposits associated with hydrothermal vents on the seafloor[2-7,110,111] has prompted the examination of marine electrical methods to map such deposits, as has been done on land for many years. Relatively little is known of either the surficial or subsurface extent of sulfide deposits, and electrical methods offer a possible way to determine such parameters. The conductivity of massive sulfides can be several times that of the basaltic host rock, and substantial resistivity anomalies are possible.

The use of electrical methods at sea has been only recently attempted in any concerted effort. The first use of electrical methods at sea was in the Red Sea, where SP anomalies up to 200 mV were recorded from the metalliferous sediments.[112] Corwin et al.[113] demonstrated the feasibility of a towed resistivity array device over a known sulfide body in shallow coastal water. A deep-ocean towed array was used in 1970 over submarine sediments in the Atlantic Ocean with marginal success.[114] A marine Schlumberger array with a surface-towed audiomagnetotelluric system was used to map known copper veins in the Great Lakes, but the anomalies were strongly affected by bottom topography.[115]

The first electrical measurements near a known deep-sea hydrothermal vent site were carried out as part of the RISE[2] program over the East Pacific Rise at 21°N.[116,117] The electrical conductivity structure of the ocean crust near the 21°N vent site was measured using an active source method. A surface vessel towed a transmitter cable consisting of an 800-m-long dipole near the seafloor, through which an AC current was passed (70 A peak). A separate receiver with two orthogonal, 9-m antennas was placed on the seafloor to detect the horizontal components of the generated electrical field. The transmitter and receiver were separated by 19 km. Results of this experiment show that a conductivity of 0.004 S/m fits the data and suggests that the high conductivity measured in surface rocks does not continue at depth.[118] The data are nonunique, and several models can fit the observed measurements; however, it appears that each of the models considered requires a low-conductivity layer between depths of 1 and 20 km.

In a similar experiment, a device known as MOSES (magnetometric off-shore electrical sounding) has also been used to measure the electrical resistivity of oceanic basalt and sediments.[108,119] MOSES consists of a vertical bipole (cable) from the sea surface to the seafloor, through which an AC current is passed (20 to 25 A at various frequencies of 0.01 to 0.25 Hz). The separate receiver, which rests on the seafloor, uses two orthogonally mounted fluxgate magnetometers to measure the horizontal component of the magnetic field induced by the AC current (see Figure 4). The bipole is towed away from the receiver to image increasingly deeper portions of the crust. The MOSES method was used to measure the resistivity of basalt and overlying sediment at two sites in Middle Valley, the sedimented spreading center of the northernmost segment of the Juan de Fuca Ridge. The resistivity of the 1800-m-thick sediment layer at site 1 was found to be 0.82 Ω/m compared with the basement basalt resistivity at site 2 of 8.5 Ω/m, where the sediment thickness was only 200 to 300 m.[108] These values are consistent with results from DSDP hole 504B, where fractured basalt resistivity ranged from 5 to 30 Ω/m.[118,120] Porosity estimates of as high as 60% at the surface, decreasing to 20% at the base of the sediments and 8% for the basalt, are in the range expected from seismic and borehole measurements.[108]

Recently, a number of detailed electrical surveys have been carried out over hydrothermal sites on the East Pacific Rise,[107] the Juan de Fuca Ridge,[121] and the Galapagos Rift.[101] Electrical resistivity measurements were made over two sulfide sites and two basalt sites on the East Pacific Rise at 12°42′N using the submersible CYANA and a 50-m cable with six electrodes.[107] In the active mode, current was passed through the current electrodes and voltages were measured at the potential electrodes, giving a measurement of resistivity. In the passive mode, voltages were measured with no current flowing through the current electrodes to measure the SP response. The cable was laid out along the seafloor by the submersible and lifted up into the water column for seawater measurements and cal-

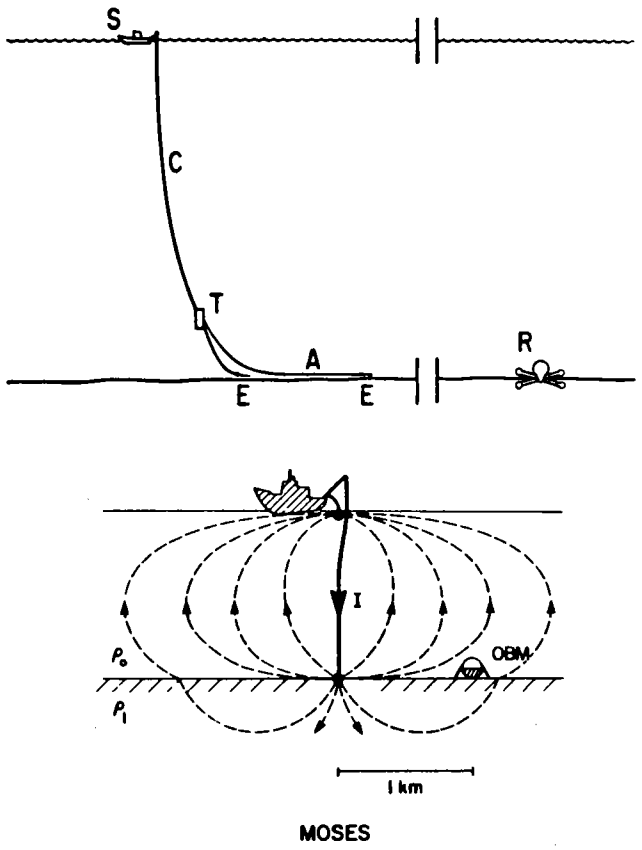

FIGURE 4. Transmitter-receiver configurations for marine electrical prospecting systems. Electrical system after Young and Cox;[117] magnetometric system (MOSES) after Nobes et al.[108]

ibration (see Francis[107] for details). The results show that the resistivity over the sulfides ranged from 0.17 to 2.13 Ω/m, compared with values of 9 to 13 Ω/m over the basalts. SP anomalies of 9.9 and 0.7 mV were measured over the two sulfide sites and no detectable SP anomalies were measured over the basalt sites. The resistivity measurements were used to estimate a thickness of 9 m for the sulfide deposit. The basalt resistivity values are consistent with other measurements of crustal resistivity,[118,120] and the highly conductive sulfides demonstrate the feasibility of such measurements on the seafloor.

In a different approach, resistivity measurements were attempted over the Juan de Fuca Ridge at the Endeavour hydrothermal site with the MINI-MOSES system.[121] The MINI-MOSES system is based on the magnetometric resistive method (MOSES) described above,[119] but uses a self-contained seafloor transmitter and a separate seafloor receiver. A submersible is required to move the receiver and transmitter to different separation distances to allow the imaging of successively deeper layers. Unfortunately, only two data points were obtained, giving a half-space resistivity of 14 Ω/m, but the viability of the technique was demonstrated.

Both of the detailed surveys described above required the use of deep-diving submersibles, which is a cumbersome and time-consuming use of a very scarce resource. The necessity of using a submarine also limits the size of the area that can be surveyed. There is also a problem with topographic noise, which can introduce considerable scatter to the measurements.[115] In an effort to address these problems, Edwards and Chave[122] and Cheesman et al.[123] present analyses of time-domain EM systems that may offer a relatively rapid and reconnaissance-style mapping tool, similar to the airborne EM systems used today on land. Transient electromagnetic systems involve the use of a "fast-on" transmitted signal and the measurement of the response picked up by the receiver. There are a number of different types of EM systems (see Figure 5), but only the horizontal coaxial magnetic dipole-dipole (HRHR) or electric dipole-dipole (ERER) systems are suited to marine environments where the seafloor is less conductive than seawater (the most common case).[123] In these systems, the initial transient is indicative of the seafloor conductivity and the later transient arrival is a measure of the seawater conductivity. If the seafloor is more conductive than seawater (as in the case of some sulfides), then the vertical coplanar magnetic dipole-dipole (HZHZ) or the vertical magnetic field of an electric dipole (EPHIHZ) systems are also useful (see Figure 5). This recent work shows great promise in the design and implementation of a marine EM reconnaissance system for seafloor mapping and exploration.

D. Seismic Methods

The seismic method involves the propagation of acoustic waves through the earth, which to a first approximation is an elastic medium. Seismic information comes both in the form of natural earthquake activity and as a result of imaging the

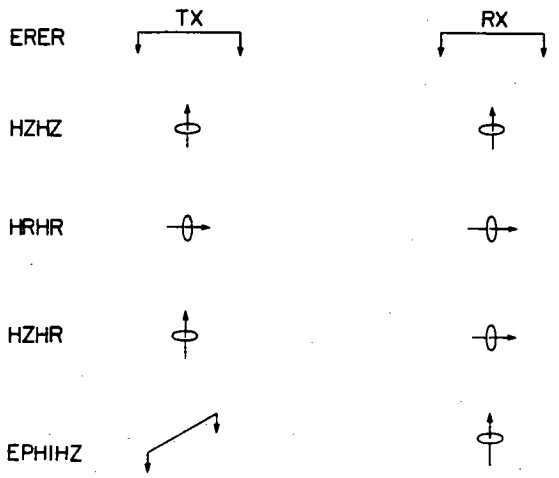

FIGURE 5. Various transmitter-receiver configurations of time-domain electromagnetic systems. After Cheesman et al.[123]

interior of the earth by active sources (i.e., reflection and refraction seismology). Microearthquake activity on land has been linked to hydrothermal activity at several geothermal systems. Shallow-focus microearthquakes of low magnitude (<2.0 Richter) have been noted at Imperial Valley,[124,125] the Rio Grande Rift zone,[126,127] and southwestern Iceland.[128-130] At Yellowstone, hydrothermal activity has been seen to be dependent upon the release of tension in the form of earthquakes, with the frequency of geyser eruptions controlled by earthquake activity, among other causes.[131] Microearthquake activity has also signaled changes in hydrothermal activity,[132,133] as well as being induced by the withdrawal of geothermal fluids.[134]

Oceanic microearthquake activity is often located along spreading centers and transforms[135,136] as well as along subduction zones. Mid-ocean ridge microearthquake activity generally occurs at shallow depths due to the thin crust and elevated isotherms present at spreading centers.[137,138] Faster-spreading ridges appear to be seismically quiet when compared with slower-spreading ridges. A number of detailed studies have revealed, however, that fast-spreading ridges have significant microseismic activity.[139] The possible contribution of hydrothermal activity to microearthquake activity was suggested by Macdonald and Mudie[139] and was investigated by Reidesel et al.[140] at the East Pacific Rise 21°N hydrothermal vent site. In this survey, five on-bottom seismometers (OBS) were deployed within 3 km of the active hydrothermal vent site, with two devices as close as 300 m. The seismic activity that was measured consisted of very small-magnitude events (0 to 1 Richter), with a maximum depth of 2 to 3 km. Harmonic tremors were also detected at this location, which were similar in character to that observed near terrestrial volcanoes (e.g., Mt. St. Helens), which may be due to subsurface magma movement associated with volcanic activity.[140] In contrast, a study over the TAG area of the Mid-Atlantic Ridge found, surprisingly, no association of microearthquake activity with known areas of hydrothermal activity.[141] Clearly, more data need to be collected to establish whether a correlation exists between hydrothermal and microearthquake activity. The exact relationship and possible physical mechanisms of these processes are ambiguous at the present time.

The effect of hydrothermal activity on the general acoustic noise level in the vicinity of an active system is also of interest. Reidesel et al.[140] measured high acoustic noise levels on the OBS sites proximal to the vent sites on the East Pacific Rise. A similar high ambient acoustic noise level was also reported by Bibee and Jacobson[142] and Jacobson et al.[143] in an OBS study of Axial seamount on the Juan de Fuca Ridge at 46°N. In this study they found that a low-temperature vent site produced anomalous noise, but another black smoker site showed no evidence of anomalous acoustic noise. These studies show more activity near the low-temperature vent sites compared with the high-temperature vents, perhaps suggesting more subsurface activity at low-temperature sites.[143] The measurement of noise spectra has been proposed as a method of detecting changes in fluid flow and hydrothermal activity.[144] This kind of measurement requires coincident monitoring of vent activity as well as microearthquake activity. At what point microearthquake activity influences vent output, however, remains largely speculative.

The locations of microearthquakes have such large error bars compared with the size of individual vent sites that it precludes the use of earthquake activity from locating as yet undiscovered vent systems. The future study of earthquake activity as it relates to hydrothermal activity requires long time-series measurements not currently available and points to a long-term observatory type of monitoring of vent activity.

E. Acoustic Methods

A number of different types of acoustic swath-mapping techniques have been developed in the last 2 decades, with the evolution of primitive side-scan sonar tools into sophisticated seafloor mapping systems. Early systems were towed both at the sea surface for rapid acquisition of low-resolution data — Geological Long Range Inclined Asdic (GLORIA)[145] and near the bottom for higher resolution of much smaller-scale features (DEEPTOW).[146] GLORIA (Mk II version) can be towed at speeds of 6 to 10 knots, with a swath width as wide as 30 km. At the 2000- to 3000-m depth of most spreading centers, the individual pixel size of a GLORIA image approaches 50 m, and while useful for establishing the geological context of the ocean floor, this system has not played a role in the discovery or mapping of hydrothermal systems.

The high-resolution (110 kHz) side-scan on Scripp's DEEPTOW instrument, however, has been involved in the study of submarine hydrothermal systems since their discovery.[47,146] At the Galapagos Rift, side-scan images were coupled with bottom photography, narrow-beam echo sounder, sub-bottom profiler, and CTD and water sampling to characterize the large-scale hydrothermal deposits (''mounds'') that occur off-axis in this region.[47,51] These mounds are 10- to 20-m-high deposits that are 50 m wide and can be several kilometers long, parallel to the axis of spreading, and at this location are found on sedimented crust between 0.5 and 0.7 m.y. in age. Side-scan sonar images were particularly effective in defining these structures, because of both their relief above the surrounding sedimented terrain and because the Mn-encrusted outer layers of the mounts were very effective acoustic backscattering targets. Subsequent sampling of the mounds has shown them to be complex depositional/diagenetic structures, formed off-axis by the circulation of hydrothermal fluid discharging through the sediments, from the underlying basement rocks. The mineral precipitation from the venting fluid and diagenesis of the surrounding sediments provides the bulk of the internal material of the mound.

Because most ''hard rock'' spreading centers represent such rugged terrain and the basement rocks have very limited acoustic backscatter contrast with hydrothermal deposits, side-scan

sonar has not been very useful in identifying and characterizing hydrothermal processes in "normal" spreading centers. Where the spreading centers are sedimented, however, side-scan techniques can be most effective in finding and mapping hydrothermal deposits. Early work on the sedimented Guaymas Basin hydrothermal field demonstrated the usefulness of this technique.[146,147] In addition, at the extremely well-studied Middle Valley site on northern Juan de Fuca, a type of side scan known as SeaMARC (both versions I and II)[148-150] played a major role in defining the hydrothermal processes at work in this sedimented spreading center.

Middle Valley is a recently abandoned spreading center at the northern end of the Juan de Fuca Ridge, with a turbidite-derived sediment cover that can reach a thickness in places in excess of 2 km. Davis and Lister[38] have shown that this sediment-filled valley is an area of very high heat flow, and argued that the subsequent restricted hydrothermal circulation has raised crustal temperatures in excess of 300°C. These proposed high crustal temperatures are supported by the sea-surface magnetic anomaly data, which show that although located within the Brunhes normally magnetized zone, the valley is overlain with a negative magnetic anomaly — presumably due to thermal or chemical demagnetization of the crustal rocks.

Although the thick sediment cover provides an insulating blanket for the underlying high-temperature rocks, fissures within the sediment floor near the outer boundaries of the valley appear to be controlling the access of hydrothermal fluids to the surface. Using SeaMARC I and II side-scan images[23,151] discovered large mound-like structures near the boundary faults, which proved to be composed of sulfides of hydrothermal origin (see Davis et al.[23] for a review of this data). The mounds were observed to be directly associated with the boundary faults (see Figure 6a) and located in areas of anomalously high heat flow of 5 to 50 W/m.[23,152] The interior of the mounds has been sampled by both piston core and diamond drilling, and it is composed of alternating beds of coarse-grained clastic sulfides and black sulfidic muds.[23,153] These sulfide deposits are large (see Figure 6b), averaging 50 m in height and roughly 500 m in diameter, and may be the largest known hydrothermal deposits in the marine environment.[23] Originally identified by SeaMARC images and later observed in the SEABEAM coverage over the same area,[154] the mounds in Middle Valley represent a geological feature that is a prime candidate for geophysical exploration.

F. Gravity Methods

The use of gravity in geophysical studies is based on the measurement of small variations in the gravitational potential field of the earth. These small-scale variations in the main gravity field are caused by lateral variations in the density distribution of the crust of the earth. These density differences can result from anomalous bodies, such as high-density orebodies or zones of alteration filled with low-density alteration minerals. Density differences also arise from the bulk porosity structure of the rock, large-scale temperature anomalies, and the presence or absence of fluid in the pore spaces. Gravity, in general, provides information about the subsurface tectonic structure and geologic setting of the underlying crust. Surface gravimeters have been used on land successfully to explore and map ore bodies and to define the regional geologic setting.[102] Gravity has also been used to determine subsidence rates due to exploitation (fluid removal), such as at the Wairakei geothermal field in New Zealand,[155] and to document caldera uplift, such as that at Long Valley, CA.[156]

Marine gravity measurements at the sea surface are distant from the source, which results in the attenuation of the high-frequency components of the gravity field signal. Near-bottom studies can overcome this problem, but other problems arise, such as an accurate knowledge of position, accurate determination of the mass distribution in the local terrain around the submersible, and the stability of the submarine or platform (which can be actually better than at the sea surface). The expected gravitational anomalies associated with hydrothermal vents are far from clear and remain a relatively unexplored area of investigation. The relatively small scale of the vents means that if any gravity signal is present, it would be attenuated at the sea surface, requiring near-bottom measurements for detection. The only high-resolution, near-bottom gravity measurements to date were carried out as part of the geophysical experiments over the ridge crest of the East Pacific Rise at 21°N.[2,157] In this survey, 20 gravity measurements were taken by a Lacoste-Romberg meter from inside the submersible DSRV Alvin along a 7-km profile across the axis of the ridge. The corrections to the data included taking into account both the overlying water mass and the variations in local terrain to produce a free-water anomaly and Bouger anomaly. The free-water anomaly shows a correlation with the bathymetry, whereas the Bouger anomaly shows a 1.5-mgal low over the neovolcanic zone. Luyendyk[157] argues, largely from ideal body modeling, that the source of this anomaly must be in the upper 2 km of crust, and so does not represent an anomaly due to a magma chamber. The small negative anomaly may, in fact, be due to the presence of hot seawater within crustal fractures in the neovolcanic zone.[157] This hypothesis fits the data, but is speculative. The corrections to the data were in some cases larger than the resultant anomaly — certainly more information is needed before this hypothesis can be confirmed. Gravity variations can occur due to fluid conditions at depth; for example, at Wairakei hydrothermal field, the gravity data show an increase in the upper steam zone to compensate for fluid drawdown by geothermal power extraction.[155]

Gravity measurements are inherently nonunique and can only suggest a number of possible models to explain the observed anomalies, limiting the usefulness of gravity data. Gravity measurements are also time-consuming to make and not an efficient use of the submersible. However, the information gained is

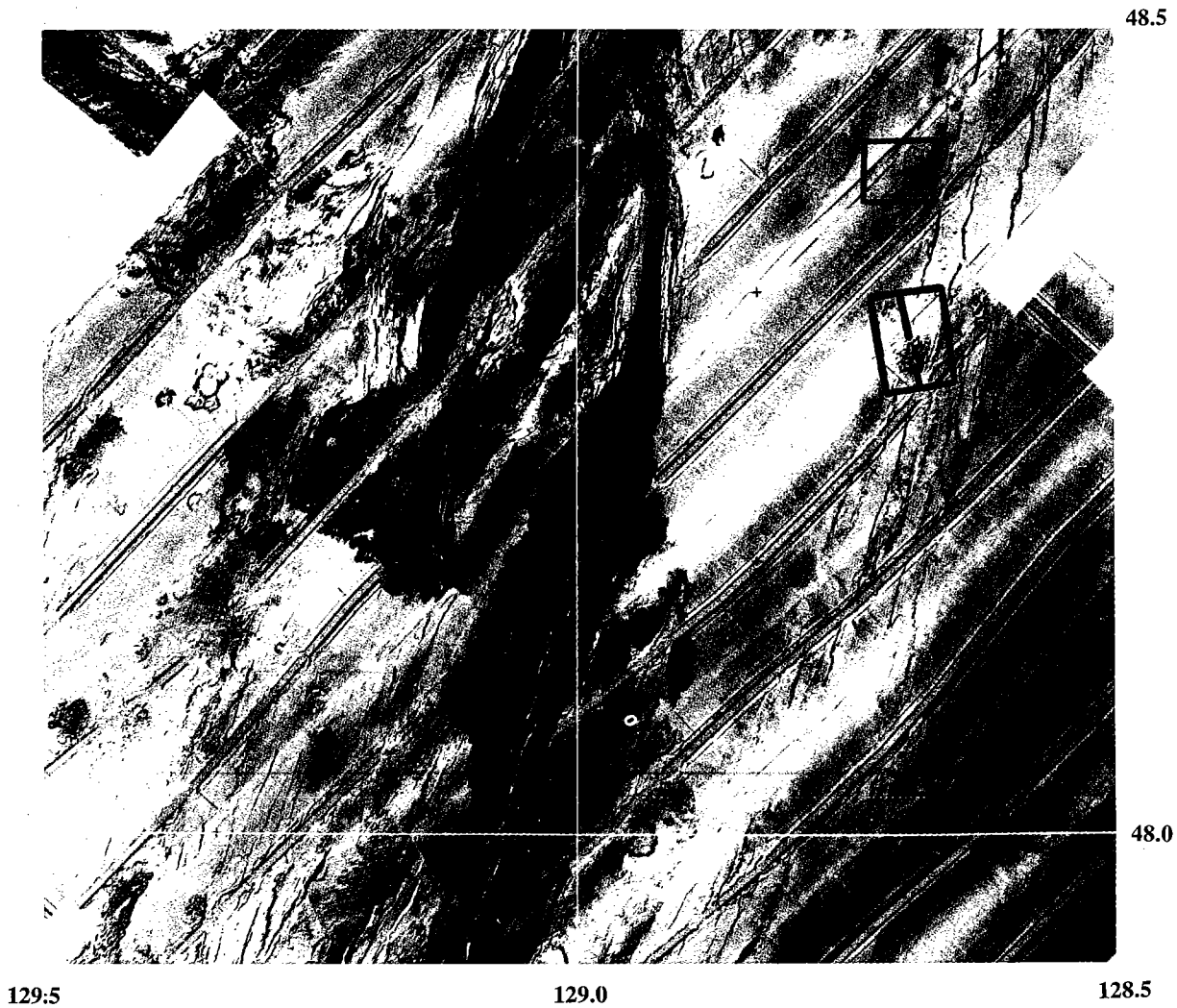

FIGURE 6. (A) SeaMARC II backscatter image mosaic of the northern Juan de Fuca Ridge/Middle Valley region. The outlined polygons show the location of hydrothermal mound sites on the eastern side of Middle Valley. (B) SeaMARC I backscatter image of hydrothermal mounds located along the fault scarps of eastern Middle Valley, on the northern Juan de Fuca Ridge. (From Davis, E. E., Currie, R. G., Riddihough, R. P., Ryan, W. B., Kastens, K., Hussong, D. M., Hammond, S. R., and Malahoff, A., *Eos Trans. AGU*, 65, 1110, 1984. With permission.)

certainly revealing and, along with other data, will help in the long-term understanding of hydrothermal vents and processes.

III. DISCUSSION

The previous section discussed the various techniques that can and have been used to study oceanic vents. Submarine vents, however, are integrated systems that by their nature are dynamic and complex features. It should be apparent that no single geophysical technique can characterize a hydrothermal vent system, but when used together with other methods, a more fundamental understanding of the system will be forthcoming. Current knowledge and measurements of vent systems have been limited to the surface features, but it is the subsurface environment that could have a greater impact upon geophysical signals. For ease of discussion, and because the substructure under mounds in a sedimented region must be very different from that under an unsedimented area, we will divide hydrothermal systems into those that exist at sedimented spreading centers and those at unsedimented spreading centers. This division is somewhat artificial, since the two systems must share common features and geological processes.

FIGURE 6B

A. Unsedimented Spreading Centers

The surface features of hydrothermal deposits have been studied and sampled in some detail, and examples of the full range of new, mature, and dead vent sites have been tentatively identified and sampled. Detailed descriptions of vent spire structures from the East Pacific Rise are contained in RISE,[2] Styrt et al.,[158] Haymon and Kastner,[159] Hekinian et al.,[160] Alt et al.,[161] and McConachy et al.[162] In the northeast Pacific, hydrothermal structures have been described on Explorer Ridge,[163] the northern Juan de Fuca Ridge,[6,98,110] the Axial Seamount,[164] and the southern Juan de Fuca.[165,166]

Data and observations on the subsurface features of a hydrothermal system are sparse, however, and largely limited to drill-hole cores[66] and subaerial exposures of ophiolite suites.[167,168] On the Galapagos Rise, submersible dives discovered a unique seafloor outcrop of hydrothermal stockwork below a sulfide deposit that had been exposed by tectonic faulting.[101] This outcrop consisted of a series of anastomosing pipes or sheets of highly altered material, enclosed by zones of extremely fractured but largely unaltered rocks. The central core of the stockwork zone consisted of altered pillow basalts, which were bleached white to pale grey,[101] very similar to the alteration "halos" that have been mapped adjacent to sulfide deposits in Cyprus and elsewhere,[168,169] and adds credibility to the application of ophiolite models of subsurface structure to seafloor hydrothermal systems. Geophysics provides the main tool to map and characterize this subsurface regime of a vent system, short of explicitly drilling the vent site.

In order to study the vent system in a coherent fashion, a working model of the system is needed. A number of models have been published that are based on submersible observations and detailed analysis of the mineralogy and textures of recovered sulfide samples (see, for example, Goldfarb et al.,[170] Hekinian and Fouquet,[171] and Tivey and Delaney[6] for unsedimented spreading centers; Lonsdale and Becker[44] for the sedimented environment). These models have implications for the resultant geophysical signals, which are likely to change as the vent system evolves. Using a generalized model of vent formation and evolution based on these published models[6,170,171] and personal observations,[172] the effects upon the geophysical signals can be assessed.

Figure 7 shows a proposed sequence for the development of the mature hydrothermal field, similar to that observed on the Explorer[163] and northern Juan de Fuca spreading centers.[6,110] These deposits are similar in form but much larger in scale than those described in the sedimented Guaymas Basin, which were also formed from coalescing sulfide chimneys.[44] In the initial stages (see Figure 7a) the onset of hydrothermal activity, which is usually localized by fissure patterns, forms small discrete vents directly on top of basalt. These high-temperature vents would produce local but intense water column temperature anomalies. The subsurface structure is relatively undeveloped, with little or no alteration of the host rock and no stockwork zone formation. This would suggest that little or no electrical or magnetic signal would be expected. Crustal seismic velocities would be expected to show little or no change from normal unaltered basalt.

As the vents become established, basal mounds begin to form, initially composed of debris from the collapse of chimneys or sedimentary fallout from hydrothermal precipitates.[159,170] Individual vents progressively coalesce into elongate ridges along the strike of a fissure (see Figure 7b).[6] The formation of a stockwork zone and significant host-rock alteration adjacent to subsurface fluid conduits most likely begins at this stage.[170] The effects of host-rock alteration may be detectable by near-bottom magnetics as the titanomagnetite in the basalt becomes altered and replaced by less magnetic minerals. As the basal mounds grow, the deposition of sulfides, both internally and externally, will produce local electrical conductivity and SP anomalies, and possibly near-bottom gravity anomalies. The seismic velocity structure under a vent site will change as voids in the previously fractured basalt become filled and replaced with hydrothermal minerals. Actively depositing vents with significant coherent deposits of pyrrhotite could give rise to strong, local, positive magnetic anomalies. In this stage, the presence of numerous venting chimneys would produce a thermal and effluent plume detectable at a distance of several kilometers.

In the mature stage, adjacent linear ridges of sulfide deposits will have further coalesced to form a roughly equidimensional field (see Figure 7c), most likely by the collapse of chimneys and unstable edifices.[163] Individual vent orifices are no longer constrained to lie exactly above the underlying fissure, since a complex plumbing system within the basal deposit can cause the fluid to exit anywhere on the surface of the mound. At this stage, the waning hydrothermal activity may no longer produce a vigorous thermal or particulate plume.[6,170,171] An extensive stockwork zone and alteration zone will likely exist beneath the surface deposits, allowing possible magnetic, gravity, and seismic anomalies to be detected at greater distances. The combination of a complex internal mound structure, the alteration of unstable mineral phases, and mass wasting of the chimney edifices may destroy any fine-scale magnetic anomalies due to pyrrhotite present in the earlier stage of development.

While somewhat speculative, the model of subsurface structure shown in Figure 7d is consistent with that observed in subaerially exposed sulfide deposits such as at Cyprus (i.e., Agrokipia Mine[89]). Certainly the general features of this model are present in some existing large submarine deposits. Specifically, and starting from the deepest features of Figure 7d, the stockwork shown in that figure represents what must be a complex feeder zone, generally controlled by the faulting and fissuring that was exposed at the original basalt surface. However, the "self-sealing" nature of hydrothermal fluids, when they mix with seawater and precipitate anhydrite and sulfide deposits, can cause this feeder zone to be much more complex

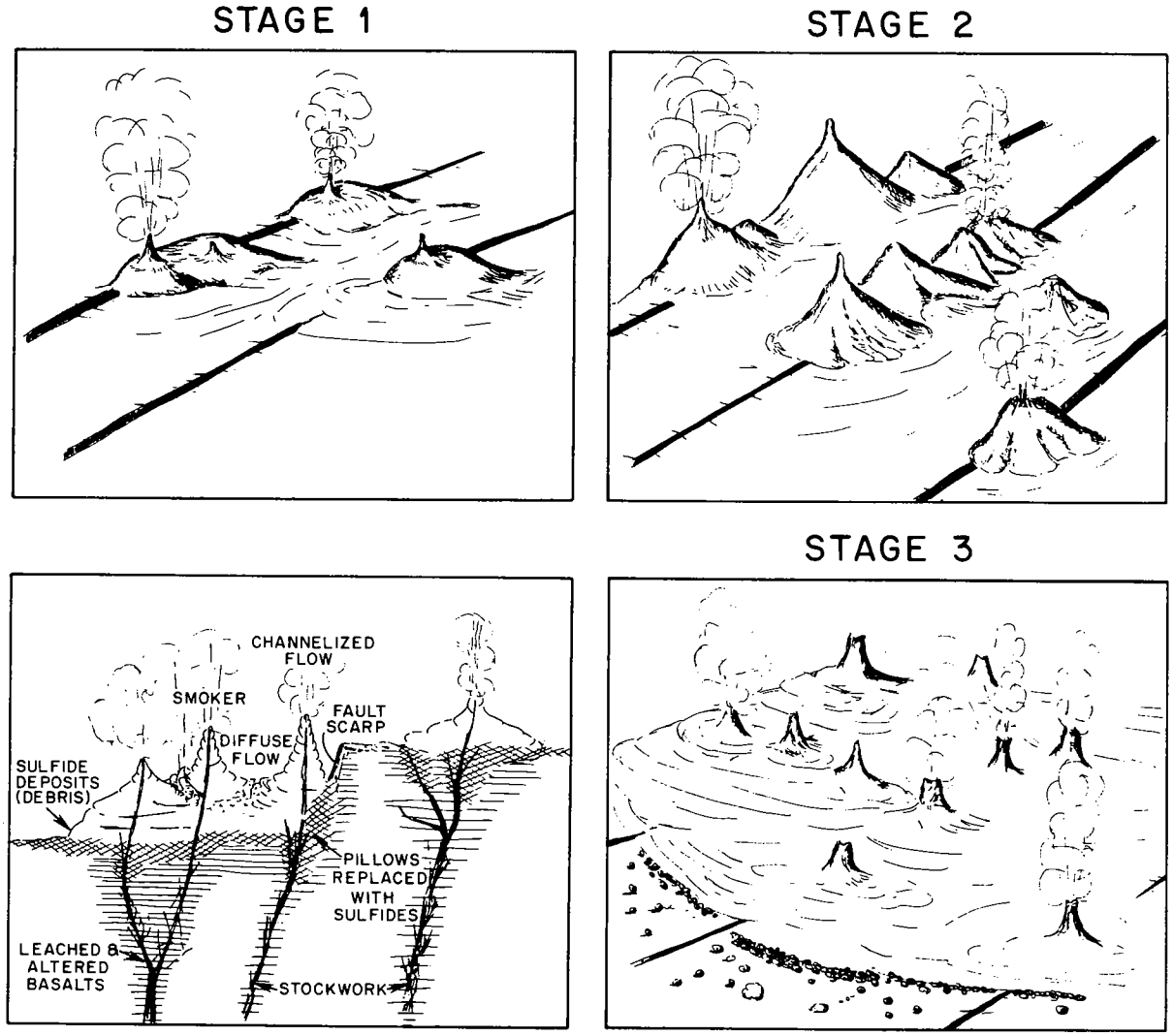

FIGURE 7. Evolutionary sequence of a hydrothermal deposit at an unsedimented spreading center. (a) Initial stage showing small discrete vents located over existing fissure structure. (b) Established stage showing coalescing structures along the fissure direction. (c) Mature vent field showing a large equidimensional deposit. (d) Subsurface model of an active hydrothermal vent system showing the relationship between the surface vents and subsurface features.

and tortuous than the pathway provided by the original fissure.

Higher in the subsurface structure of the hydrothermal system, leached extrusive basalts that form an alteration "halo" around the main sulfide deposit are a common feature of such deposits.[89] This alteration halo was well developed around the Agrokipia A deposit surveyed in some detail in Cyprus, and provided a strong magnetic (an anomaly low) signature in contrast to the surrounding unaltered rocks.[89] Above the leached and unpigmented alteration halo, sulfides can completely replace the extrusive rocks, forming in some cases sulfide "pillows" that are pseudomorphic after the original pillow basalts.[168] Above the replacement pillows lies the bulk of the sulfide deposit, generally formed of sulfides (pyrrhotite, pyrite, sphalerite, and chalcopyrite) and their alteration products, silica, and biological debris. Capping the structure are the very dramatic constructional chimneys, which can reach to heights of several tens of meters above the upper surface of the mounds. Although the highest temperature fluid is very channelized and exits from the summits and upper flanks of the spires, a substantial amount of lower-temperature fluid has been observed as diffuse venting from large areas over the surface of the basal mound (see Figure 7d).[6,63,171] This diffuse venting is thought to be responsible for a large portion of the heat and mass flux from a mature hydrothermal system[63] and supports a large biological population.[173] The relative proportions of mass and heat flux between the channelized flow and the diffuse flow are important parameters, but have not been determined.

The rate at which hydrothermal deposits grow and evolve

are fundamental parameters for which there are only limited data. Individual spire growth rates on hydrothermal structures have been estimated from repeated submersible observations (30 cm/d[160,170]) and from time-lapse camera observations (3 cm/d[174]; 10 cm/d[175]). The rate at which the general hydrothermal field grows is completely unknown. The "style" in which this growth occurs, however, can be inferred from observations of a variety of vent deposits in different stages of their evolutionary cycle. The deposits on Explorer Ridge were particularly useful in this respect.[163,172] On Explorer Ridge, the deposits were systematically younger from south to north, with hydrothermal activity following a large-scale crustal cracking front that was progressively propagating northward.

After a hydrothermal deposit reaches maturity and fluid flux ceases, it is not clear how long these sulfide deposits remain on the seafloor as identifiable structures. The sulfide minerals that form the deposits are not in chemical equilibrium with near-bottom seawater and will react to form new minerals.[170] On the Explorer Ridge, standing sulfide deposits that were no longer venting fluid showed clearly visible signs of alteration (e.g., red staining on the surface, broken spires, and a rounded, much less angular surface than active vents). In the southern (oldest) part of the Explorer Rift valley, the only remaining hydrothermal features were large, flat, "pond-like" deposits of amorphous reddish-orange material, presumably iron oxyhydroxides and silica, insoluble remnants of an original sulfide deposit. Without the protection of a heavy sediment cover or the benefit of being covered by a fortuitous volcanic eruption, the death and decay of a hydrothermal deposit may be as rapid as its growth.[158,159]

B. Sedimented Spreading Centers

Spreading centers that are physically close to continents and exposed to extremely high sedimentation rates form a small but extremely interesting class of geological structures. Guaymas Basin in the Gulf of California, Escanaba Trough in the southern Gorda Ridge, and Middle Valley on the northern Juan de Fuca Ridge are the three most studied sedimented spreading centers. In Guaymas, hydrothermal circulation seems to be directly associated with shallow-level (within the sediment column) dike and sill intrusions,[44] and at Escanaba, hydrothermal deposition is related to large-scale volcanic dome emplacement within the axial valley.[176] The large-scale hydrothermal deposits located in Middle Valley are controlled by the tectonic bounding faults at the edge of the valley, and do not appear to be related to current volcanic activity.[23]

Inundated by thick insulating sediments, the crustal volcanic rocks at these spreading centers are not rapidly cooled by the free, open convection of seawater that occurs at unsedimented spreading centers. In addition to retaining crustal heat longer (perhaps 100,000 times longer) than normal oceanic crust, limited access to the surface through tectonic fissures in the sediment cover can channelize the hydrothermal circulation that does occur. This stabilization of the hydrothermal flux in one location for long periods can result in sulfide deposits that are orders of magnitude larger than those that occur at unsedimented spreading centers.[23,177] Both the long-term heat retention and the large-scale hydrothermal deposits result in characteristic geophysical signatures; these include high heat flow within the sedimented area, large-scale magnetic anomaly lows associated with the high-temperature crustal alteration, and anomalous acoustic backscatter.[23,44,176] In addition, rapid sedimentation can cover and protect the large sulfide deposits from oxidation after formation, and the proximity to a continent can provide the opportunity for later obduction into the subaerial environment. Buried sulfide bodies would be ideal targets for electrical prospecting methods, and if pyrrhotite is a major component,[23,44,174,177] near-bottom magnetics would also show anomalous bodies (see Figure 8). Near-bottom gravity could also locate buried sulfides due to the high-density contrast of sulfides compared with sediments.

The formation dynamics and subsurface structure of a sedimented hydrothermal deposit are even more speculative and based on less data than unsedimented spreading centers. While it is possible to predict what geophysical signals should be present at a sedimented spreading center hydrothermal deposit, fundamental unknowns, such as the deposit thickness, the composition at depth, the digenesis of the underlying sediment, the replacement by sulfides, and even the basic processes associated with sulfide body accretion keep these predictions in the speculative category. Clearly, more study is needed to characterize the geological processes that are taking place.

IV. CONCLUSIONS

In conclusion, the discovery of oceanic hydrothermal vents has confirmed early ideas of active convection within the oceanic crust and radically changed ideas on heat and chemical fluxes within the oceans and crust. Many questions remain, however; for example, the subsurface extent of a vent field is relatively unknown. Geophysical techniques can provide tools to study this environment. The magnitude of the diffuse heat flux remains a difficult problem to quantify; only by careful accounting of all the mass and energy fluxes can this variable be ascertained. Accurate determination would require a significant monitoring network. Little is known about the time-series behavior of vents, whether they are episodic or steady state. These questions can only be answered by repeated vent-site visits and long time-series measurements. A whole suite of concurrent geophysical measurements would go a long way toward refining models of vent structure and evolution. The logical extension of this is the exciting possibility of establishing a long-term observatory on the seafloor at a vent site,[178] which could begin a new era in the interdisciplinary study of the ocean basins.

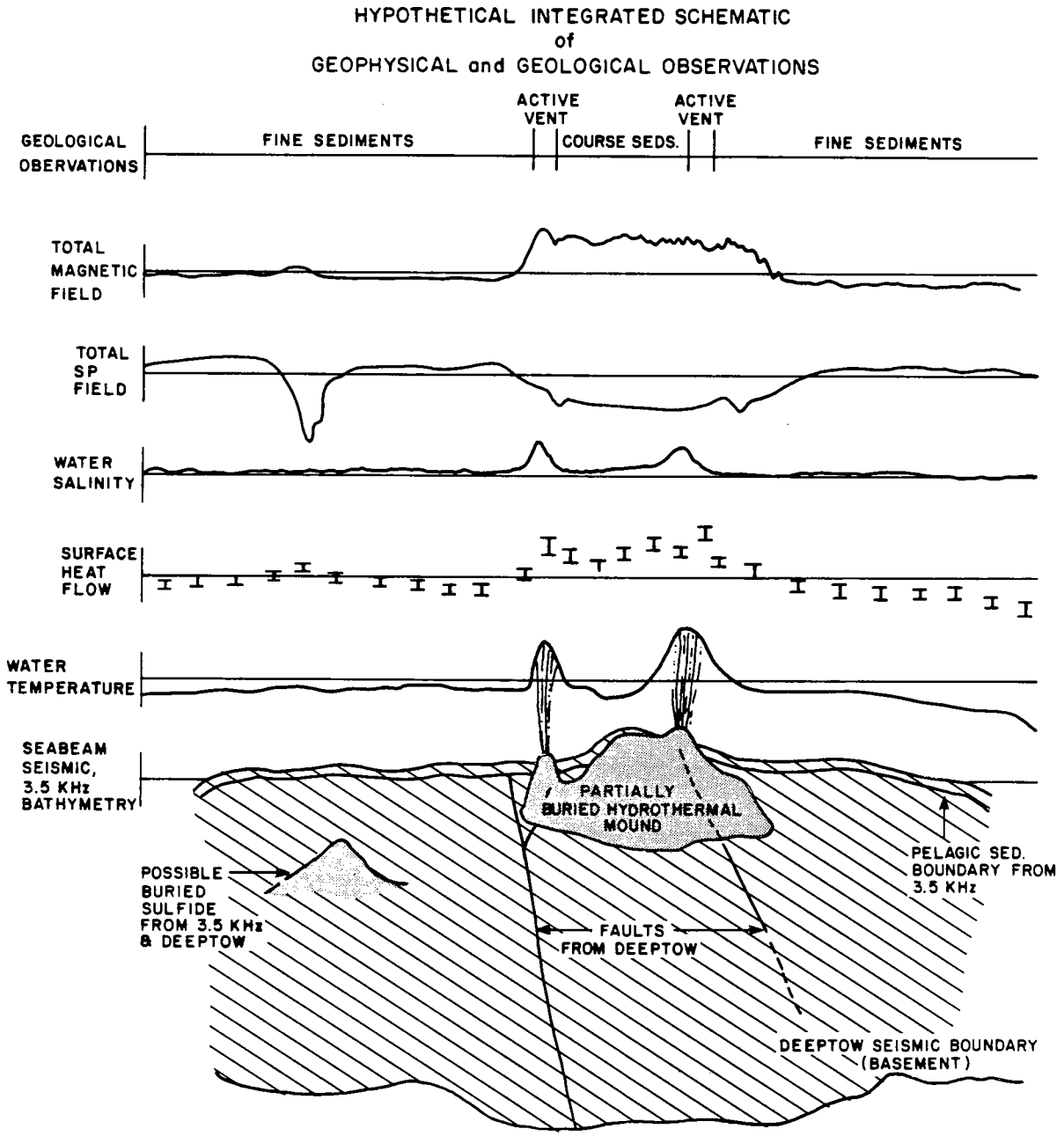

FIGURE 8. Geophysical survey over a sedimented, spreading-center mound showing possible geophysical anomalies in response to buried sulfide deposits.

REFERENCES

1. **Edmonds, J. M.,** Ridge crest hot springs: the story so far, *Eos*, 61, 129, 1980.
2. RISE group, East Pacific Rise: hot springs and geophysical experiments, *Science*, 207, 1421, 1980.
3. **Hekinian, R., Fevrier, M., Bischoff, J. L., Picot, P., and Shanks, W. C.,** Sulfide deposits from the East Pacific Rise near 21°N, *Nature*, 207, 1433, 1980.
4. **Malahoff, A.,** A comparison of the massive submarine polymetallic sulfides of the Galapagos Rift with some continental deposits, *Mar. Technol. Soc. J.*, 16, 39, 1982.

5. **Rona, P. A.,** Black smokers and massive sulfides at the TAG hydrothermal Field, Mid-Atlantic Ridge 26°N, *Eos Trans. AGU,* 66, 936, 1985.
6. **Tivey, M. K. and Delaney, J. R.,** Growth of large sulfide structures on the Endeavour segment of the Juan de Fuca Ridge, *Earth Planet. Sci. Lett.,* 77, 303, 1986.
7. **Franklin, J. M., Lydon, J. W., and Sangster, D. F.,** Volcanic massive sulfide deposits, in *Economic Geology,* 75th Anniversary volume, Skinner, B. J., Ed., Economic Geology, New Haven, CT, 1981.
8. **Hessler, R. S. and Smithey, W. M.,** The distribution and community structure of megafauna at the Galapagos Rift hydrothermal vents, in *Hydrothermal Processes at Seafloor Spreading Centers,* NATO Conf. Ser. IV, 12, Rona, P. A., Boström, K., Laubier, L., and Smith, K. L., Eds., Plenum Press, New York, 1983, 735.
9. **Desbruyeres, D. and Laubier, L.,** Primary consumers from hydrothermal vents animal communities, in *Hydrothermal Processes at Seafloor Spreading Centers,* NATO Conf. Ser. IV, 12, Rona, P. A., Boström, K., Laubier, L., and Smith, K. L., Eds., Plenum Press, New York, 1983, 711.
10. **Corliss, J. B., Dymond, J., Gordon, L. I., Edmond, J. M., von Herzen, R. P., Ballard, R. D., Green, K., Williams, D., Bainbridge, A., Crane, K., and van Andel, T. H.,** Submarine thermal springs on the Galapagos rift, *Science,* 203, 1073, 1979.
11. **Jannasch, H.,** Microbial processes at deep sea hydrothermal vents, in *Hydrothermal Processes at Seafloor Spreading Centers,* NATO Conf. Ser. IV, 12, Rona, P. A., Boström, K., Laubier, L., and Smith, K. L., Eds., Plenum Press, New York, 1983, 677.
12. **Glenn, M. F.,** Introducing an operational multi-beam array sonar, *Int. Hydrogr. Rev.,* 47, 35, 1970.
13. **Renard, V. and Allenou, J. P.,** SEABEAM multi-beam echo-sounding in "Jean Charcot". Description, evaluation and first results, *Int. Hydrogr. Rev.,* 56, 35, 1979.
14. **Farr, H. K.,** Multibeam bathymetric sonar: Sea Beam and Hydrochart, *Mar. Geol.,* 4, 77, 1980.
15. **Spiess, F. N. and Tyce, R. C.,** Marine Physical Laboratory deep-tow instrumentation system, S10 Ref., 73, 1973.
16. **Phillips, J. D., Driscoll, A. H., Peal, K. R., Marquet, W. M., and Owen, D. M.,** A new geological survey tool: ANGUS, *Deep-Sea Res.,* 26A, 211, 1979.
17. **Elder, J. W.,** Physical processes in geothermal areas, in *Terrestrial Heat Flow,* Lee, W. H. K., Ed., American Geophysical Union, Geophysical Mon. Ser. 8, 1965, 211.
18. **Francheteau, J. and Ballard, R. D.,** The East Pacific Rise near 21°S: inferences for along-strike variability of axial processes of the mid-ocean ridge, *Earth Planet. Sci. Lett.,* 64, 93, 1983.
19. **Rona, P. A., Klinkhammer, G., Nelsen, T. A., Trefry, J. H., and Elderfield, H.,** Black smokers, massive sulphides and vent biota at the Mid-Atlantic Ridge, *Nature,* 321, 33, 1986.
20. **Renard, V., Hekinian, R., Francheteau, J., Ballard, R. D., and Backer, H.,** Submersible observations at the axis of the ultra-fast-spreading East Pacific Rise (17°30′ to 21°30′S), *Earth Planet. Sci. Lett.,* 75, 339, 1985.
21. **Lonsdale, P., Batiza, R., and Simkin, T.,** Metallogenesis at seamounts on the East Pacific Rise, *Mar. Technol. Soc. J.,* 16, 54, 1982.
22. **Fyfe, W. S. and Lonsdale, P.,** Ocean floor hydrothermal activity, in *The Sea,* Vol. 7, Emiliani, C., Ed., John Wiley & Sons, New York, 1981, 589.
23. **Davis, E. E., Goodfellow, W. D., Bornhold, B. D., Adshead, J., Blaise, B., Villinger, H., and Le Cheminant, G.,** Massive sulfides in a sedimented rift valley, northern Juan de Fuca Ridge, *Earth Planet. Sci. Lett.,* 82, 49, 1987.
24. **Little, S. A., Stolzenbach, K. D., and Von Herzen, R. P.,** Measurements of plume flow from a hydrothermal vent field, *J. Geophys. Res.,* 92, 2587, 1987.
25. **Couten, H., Klitgord, K. D., and Whitehead, J. A.,** Segmentation of mid-ocean ridges, *Nature,* 317, 225, 1985.
26. **Macdonald, K. C., Haymon, R. M., and Perram, L. J.,** 13 new hydrothermal vent sites found on the East Pacific Rise, 20°—21°S, *Eos Trans. AGU,* 67, 1232, 1986.
27. **Parker, R. L. and Oldenburg, D. W.,** Thermal model of ocean ridges, *Nature,* 242, 137, 1973.
28. **McKenzie, D. P. and Sclater, J. G.,** Heat flow in the eastern Pacific and sea-floor spreading, *Bull. Volcanol.,* 33, 101, 1969.
29. **Sclater, J. G., Anderson, R. N., and Bell, M. L.,** Elevation of ridges and evolution of the central eastern Pacific, *J. Geophys. Res.,* 76, 7888, 1971.
30. **Von Herzen, R. P. and Anderson, R. N.,** Implications of heat flow and bottom water temperature in the eastern equatorial Pacific, *Geophys. J. R. Astron. Soc.,* 26, 427, 1972.
31. **Hyndman, R. D., Davis, E. E., and Wright, J. A.,** The measurement of marine geothermal heat flow by a multipenetration probe with digital acoustic telemetry and *in situ* conductivity, *Mar. Geophys. Res.,* 4, 181, 1979.
32. **Moran, J. E. and Lister, C. R. B.,** Heat flow across Cascadia basin near 47°N, 128°W, *J. Geophys. Res.,* 92, 11416, 1987.
33. **Talwani, M., Windisch, C. C., and Langseth, M. G.,** Reykjanes ridge crest: a detailed geophysical study, *J. Geophys. Res.,* 76, 473, 1971.
34. **Lister, C. R. B.,** On the thermal balance of a mid-ocean ridge, *Geophys. J. R. Astron. Soc.,* 26, 515, 1972.
35. **Le Pichon, X. and Langseth, M. G.,** Heat flow from mid-ocean ridges and sea-floor spreading, *Tectonophysics,* 8, 319, 1969.
36. **Williams, D. L., Von Herzen, R. P., Sclater, J. G., and Anderson, R. N.,** The Galapagos Spreading Center: lithospheric cooling and hydrothermal circulation, *Geophys. J. R. Astron. Soc.,* 38, 587, 1974.
37. **Sclater, J. G. and Klitgord, K. D.,** A detailed heat flow, topographic, and magnetic survey across the Galapagos Spreading Center at 86° West, *J. Geophys. Res.,* 78, 6951, 1973.
38. **Davis, E. E. and Lister, C. R. B.,** Heat flow measurements over the Juan de Fuca Ridge: evidence for widespread hydrothermal circulation in a highly heat transportive crust, *J. Geophys. Res.,* 82, 4845, 1977.
39. **Wolery, T. J. and Sleep, N.,** Hydrothermal circulation and geochemical flux at mid-ocean ridges, *J. Geol.,* 84, 249, 1976.
40. **Green, K. E., Von Herzen, R. P., and Williams, D. L.,** The Galapagos Spreading Center at 86°W: a detailed geothermal field study, *J. Geophys. Res.,* 86, 979, 1981.
41. **Becker, K. and Von Herzen, R. P.,** Heat flow on the western flank of the East Pacific Rise at 21°N, *J. Geophys. Res.,* 88, 1057, 1983.
42. **Langseth, M. G., Mottl, M., Hobart, M., and Fisher, A.,** Hydrothermal circulation in the vicinity of the DSDP 501/504 sites on the south flank of the Costa Rica Rift, *Eos Trans. AGU,* 67, 1222, 1986.
43. **Fehn, U., Green, K. E., Von Herzen, R. P., and Cathles, L. M.,** Numerical models for the hydrothermal field at the Galapagos spreading center, *J. Geophys. Res.,* 88, 1033, 1983.
44. **Lonsdale, P. and Becker, K.,** Hydrothermal plumes, hot springs, and conductive heat flow in the Southern Trough of Guaymas Basin, *Earth Planet. Sci. Lett.,* 73, 211, 1985.
45. **Williams, D. L., Green, K., van Andel, T., Von Herzen, R., Dymond, J., and Crane, K.,** The hydrothermal mounds of the Galapagos Rift: observations with DSRV Alvin and detailed heat flow studies, *J. Geophys. Res.,* 84, 7467, 1979.
46. **Klitgord, K. D. and Mudie, J. D.,** The Galapagos spreading center: a near-bottom geophysical survey, *Geophys. J. R. Astron. Soc.,* 38, 563, 1974.
47. **Lonsdale, P.,** Deep-tow observations at the Mounds abyssal hydrothermal field, Galapagos Rift, *Earth Planet, Sci. Lett.,* 36, 92, 1977.
48. **Abbott, D. H., Morton, J. L., and Holmes, M. L.,** Heat flow measurements on a hydrothermally-active, slow-spreading ridge: the

Escanaba Trough, *Geophys. Res. Lett.*, 13, 678, 1986.
49. **Baker, E. T. and Massoth, G. J.,** Characteristics of hydrothermal plumes from two vent fields on the Juan de Fuca Ridge, northeast Pacific Ocean, *Earth Planet. Sci. Lett.*, 85, 59, 1987.
50. **Crane, K., Aikman, F., III, Embley, R., Hammond, S., Malahoff, A., and Lupton, J.,** The distribution of geothermal fields on the Juan de Fuca Ridge, *J. Geophys. Res.*, 90, 727, 1985.
51. **Weiss, R. F., Lonsdale, P. F., Lupton, J. E., Bainbridge, A. E., and Craig, H.,** Hydrothermal plumes in the Galapagos Rift, *Nature*, 267, 600, 1977.
52. **Lupton, J. E., Weiss, R. F., and Craig, H. C.,** Mantle helium in hydrothermal plumes in the Galapagos Rift, *Nature*, 266, 603, 1977.
53. **Detrick, R. S., Williams, D. L., Mudie, J. D., and Sclater, J. G.,** Bottom water temperatures at the Galapagos spreading centre, *Geophys. J. R. Astron. Soc.*, 38, 627, 1974.
54. **Scott, S. D., Rona, P. A., McGregor, B. A., and Scott, M. A.,** The TAG hydrothermal field, *Nature*, 251, 301, 1974.
55. **Humphris, S. E. and Thompson, G.,** Hydrothermal alteration of oceanic basalts by seawater, *Geochim. Cosmochim. Acta*, 42, 107, 1978.
56. **Rona, P. A., McGregor, B. A., Betzer, P. R., Bolger, G. W., and Krause, D. C.,** Anomalous water temperatures over the Mid-Atlantic Ridge crest, *Geol. Soc. Am. Bull.*, 87, 661, 1975.
57. **Lowell, R. P. and Rona, P. A.,** On the interpretation of near-bottom water temperature anomalies, *Earth Planet. Sci. Lett.*, 32, 18, 1976.
58. **Fehn, U., Siegel, M. D., Robinson, G. R., Holland, H. D., Williams, D. L., Ericson, A. J., and Green, K. E.,** Deep water temperatures in the FAMOUS area, *Geol. Soc. Am. Bull.*, 88, 488, 1977.
59. **Crane, K. and Normark, W.,** Hydrothermal activity and crestal structure of the East Pacific Rise at 21°N, *J. Geophys. Res.*, 82, 5336, 1977.
60. **Roth, S. and Dymond, J.,** Where wafts the hydrothermal plume? A moored sensor record of lateral particle flux above Endeavour ridge, *Eos Trans. AGU*, 67, 1027, 1986.
61. **Baker, E. T., Massoth, G. J., and Feely, R. A.,** Cataclysmic hydrothermal venting on the Juan de Fuca Ridge, *Nature*, 329, 149, 1987.
62. **Macdonald, K. C., Becker, K., Spiess, F. N., and Ballard, R. D.,** Hydrothermal heat flux of the "black smoker" vents on the East Pacific Rise, *Earth Planet. Sci. Lett.*, 48, 1, 1980.
63. **Converse, D. R., Holland, H. D., and Edmond, J. M.,** Flow rates in the axial hot springs of the East Pacific Rise (21°N): implications for the heat budget and the formation of massive sulfide deposits, *Earth Planet. Sci. Lett.*, 69, 159, 1984.
64. **Macdonald, K. C.,** Geophysical settings for hydrothermal vents and mineral deposits on the East Pacific Rise, *Mar. Technol. Soc. J.*, 16(3), 26, 1982.
65. **Cathles, L. M. and Fehn, U.,** Convection processes on ridge flanks, *Eos Trans. AGU*, 66, 920, 1985.
66. **Alt, J., Honnerez, J., Laverne, C., and Emmerman, R.,** Hydrothermal alteration of a 1 km section through the upper oceanic crust, Deep Sea Drilling Project Hole 504B: mineralogy, chemistry, and evolution of seawater-basalt interaction, *J. Geophys. Res.*, 91, 10309, 1986.
67. **Vine, F. J. and Matthews, D. H.,** Magnetic anomalies over oceanic ridges, *Nature*, 199, 947, 1963.
68. **Harrison, C. G. A.,** Marine magnetic anomalies — the origin of the stripes, *Annu. Rev. Earth Planet. Sci.*, 15, 505, 1987.
69. **Banerjee, S. K.,** The magnetic layer of the ocean crust — how thick is it?, *Tectonophysics*, 105, 15, 1984.
70. **Johnson, H. P.,** Magnetization of the oceanic crust, *Rev. Geophys.*, 17, 215, 1979.
71. **Peterson, N., Eisenach, P., and Bleil, U.,** Low temperature alteration of the magnetic minerals in ocean floor basalts, in *Deep Drilling Results in the Atlantic Ocean: Ocean Crust, Maurice Ewing Series*, Vol. 2, Talwani, M., Harrison, C. G. A., and Hayes, D. E., Eds., AGU, Washington, D.C., 1979, 169.
72. **Honnerez, J.,** The aging of the oceanic crust at low temperature, in *The Sea*, Vol. 7, Emiliani, C., Ed., John Wiley & Sons, New York, 1981, 525.
73. **Thompson, G.,** Basalt-seawater interaction, in *Hydrothermal Processes at Seafloor Spreading Centers*, NATO Conf. Ser. IV, 12, Rona, P. A., Boström, K., Laubier, L., and Smith, K. L., Eds., Plenum Press, New York, 1983, 225.
74. **Mottl, M. J.,** Hydrothermal processes at seafloor spreading centers: application of basalt-seawater experimental results, in *Hydrothermal Processes at Seafloor Spreading Centers*, NATO Conf. Ser. IV, 12, Rona, P. A., Boström, K., Laubier, L., and Smith, K. L., Eds., Plenum Press, New York, 1983, 199.
75. **Irving, E., Robertson, W. A., and Aumento, F.,** The Mid-Atlantic ridge near 45°N. VI. Remanent intensity, susceptibility, and iron content of dredged samples, *Can. J. Earth Sci.*, 7, 226, 1970.
76. **Marshall, M. and Cox, A.,** Magnetic changes in pillow basalts due to sea-floor weathering, *J. Geophys. Res.*, 77, 6459, 1972.
77. **Johnson, H. P. and Merrill, R.,** Low temperature oxidation of a titanomagnetite and the implications for paleomagnetism, *J. Geophys. Res.*, 78, 4938, 1978.
78. **Johnson, H. P. and Atwater, T.,** Magnetic study of basalts from the Mid-Atlantic ridge, lat. 37°N, *Geol. Soc. Am. Bull.*, 88, 637, 1977.
79. **Thompson, G. and Humphris, S. E.,** Seawater-rock interaction in the oceanic basement, in *Proc. 2nd Int. Symp. Water-Rock Interact.*, 3, Pacquet, H. and Tardy, Y., Eds., University Louis Pasteur, Strasbourg, France, 1977.
80. **Luyendyk, B. and Melson, W.,** Magnetic properties and petrology of rocks near the crest of the Mid-Atlantic Ridge, *Nature*, 215, 147, 1967.
81. **Ade-Hall, J. M., Palmer, H. C., and Hubbard, T. P.,** The magnetic and opaque petrological response of basalt to regional hydrothermal alteration, *Geophys. J. R. Astron. Soc.*, 24, 137, 1971.
82. **Hall, J. M.,** The Iceland Research Drilling Project crustal section: variation of magnetic properties with depth in Icelandic-type oceanic crust, *Can. J. Earth Sci.*, 22, 85, 1985.
83. **Smith, G. M. and Banerjee, S. K.,** Magnetic structure of the upper kilometer of the marine crust at Deep Sea Drilling Project Hole 504B, eastern Pacific Ocean, *J. Geophys. Res.*, 91, 10337, 1986.
84. **Studt, F. E.,** Magnetic survey of the Wairakei hydrothermal field, *N.Z. J. Geol. Geophys.*, 2, 746, 1959.
85. **Studt, F. E.,** Preliminary survey of the hydrothermal field at Rabaul, New Britain, *N.Z. J. Geol. Geophys.*, 4, 274, 1961.
86. **Koenig, J. B.,** The Salton-Mexicali Geothermal Province, California Division of Mines and Geology, *Min. Inf. Service*, 20, 75, 1967.
87. **Black, H. T.,** A subsurface study of the Mesa geothermal anomaly, Imperial Valley, California, *Natl. Sci. Found. NSF.*, Washington, D.C., Rep. NSF-RA-N-75-126, 1967, 58.
88. **Ben-Avraham, Z., Shoham, Y., Klein, E., Michelson, H., and Serruya, C.,** Magnetic survey of lake Kinneret — Central Jordan Valley, Israel, *Mar. Geophys. Res.*, 4, 257, 1980.
89. **Johnson, H. P., Karsten, J. L., Vine, F. J., Smith, G. C., and Schonharting, G.,** A low-level magnetic survey over a massive sulfide ore body in the Troodos ophiolite complex, Cyprus, *Mar. Technol. Soc. J.*, 16, 76, 1982.
90. **Bjornsson, S., Arnoson, S., and Tomasson, J.,** Economic evaluation of Reykjanes thermal brine area, Iceland, *Am. Assoc. Pet. Geol. Bull.*, 56, 2380, 1972.
91. **Phillips, J. D., Woodside, J., and Bowin, C. O.,** Magnetic and gravity anomalies in the central Red Sea, in *Hot Brines and Recent Heavy Metal Deposits in the Red Sea*, Degens, E. T. and Ross, D. A., Eds., 1969, 98.

92. **Rona, P. A.,** Magnetic signatures of hydrothermal alteration and volcanogenic mineral deposits in oceanic crust, *J. Volc. Geoth. Res.,* 3, 219, 1978.
93. **Hunt, J. M., Hayes, E. E., Degens, E. T., and Ross, D. A.,** Red Sea: detailed survey of hot brine areas, *Science,* 156, 514, 1967.
94. **Macgregor, B. A. and Rona, P. A.,** Crest of Mid-Atlantic ridge at 26°N, *J. Geophys. Res.,* 80, 3307, 1975.
95. **Macgregor, B. A., Harrison, C. G. A., Lavelle, J. W., and Rona, P. A.,** Magnetic anomaly pattern on Mid-Atlantic crest at 26°N, *J. Geophys. Res.,* 82, 231, 1977.
96. **Miller, S. P.,** The validity of geological interpretations of marine magnetic anomalies, *Geophys. J. R. Astron. Soc.,* 50, 1, 1977.
97. **Tivey, M. A. and Johnson, H. P.,** A near-bottom magnetic survey over an active hydrothermal vent field: Northern Juan de Fuca Ridge, *Eos Trans. AGU,* 66, 925, 1985.
98. **Tivey, M. K. and Delaney, J. R.,** Sulfide deposits from the Endeavour segment of the Juan de Fuca Ridge, *Mar. Mining,* 5, 165, 1985.
99. **Tivey, M. A. and Johnson, H. P.,** The central anomaly magnetic high: implications for ocean crust construction and evolution, *J. Geophys. Res.,* 92, 12685, 1987.
100. **Perram, L. J., Macdonald, K. C., and Miller, S. P.,** Axial magnetic lows: implications for a shallow magma chamber?, *Eos Trans. AGU,* 67, 1232, 1986.
101. **Embley, R. W., Jonasson, I. R., Perfit, M. R., Tivey, M. A., Malahof, A., Franklin, J. M., Smith, M. F., and Francis, T. J. G.,** Submersible investigation of an extinct hydrothermal system on the Galapagos ridge: sulfide mounds, stockwork zone, and differentiated lavas, *Can. Mineral.,* 26, 517, 1988.
102. SEG, *Mining Geophysics,* Society of Exploration Geophysics, Tulsa, OK, 1966.
103. **Fountain, D. K.,** Geophysical case histories of disseminated sulfide deposits in British Columbia, *Geophysics,* 37, 142, 1972.
104. **Sato, M. and Mooney, H. M.,** The electrochemical mechanism of sulfide self-potentials, *Geophysics,* 25, 226, 1960.
105. **Telford, W. M., Geldart, L. P., Sheriff, R. E., and Keys, D. A.,** *Applied Geophysics,* Cambridge University Press, Cambridge, U.K., 1976.
106. **Archie, G. E.,** The electrical resistivity log as an aid in determining some reservoir characteristics, *J. Pet. Technol.,* 5, 1, 1942.
107. **Francis, T. J.,** Resistivity measurements of an ocean floor sulphide mineral deposit from the submersible CYANA, *Mar. Geophys. Res.,* 7, 419, 1985.
108. **Nobes, D. C., Law, L. K., and Edwards, R. N.,** The determination of resistivity and porosity of the sediment and fractured basalt layers near the Juan de Fuca Ridge, *Geophys. J. R. Astron. Soc.,* 86, 289, 1986.
109. **McNitt, J. R.,** Review of geothermal resources, *Am. Geophys. Union Mono.,* 9, 240, 1965.
110. MERGE group, Regional setting and local character of a hydrothermal field/sulfide deposit on the Endeavour segment of the Juan de Fuca Ridge, *Eos Trans. AGU,* 65, 1111, 1984.
111. CYAMEX expedition, First manned submersible dives on the East Pacific Rise at 21°N (Project Rita): general results, *Mar. Geophys. Res.,* 4, 345, 1981.
112. **Brooks, R. R., Kaplan, I. R., and Peterson, M. N. A.,** Trace element composition of Red Sea geothermal brine and interstitial water, in *Hot Brines and Recent Heavy Metal Deposits in the Red Sea,* Degens, E. T., and Ross, D. A., Eds., 1969, 180.
113. **Corwin, R. F., Ebersole, W. C., and Wilde, P.,** A self-potential detection system for the marine environment, Offsh. Tech. Conf., Houston, TX, OTC paper #1258, 1970.
114. **Brewitt-Taylor, C. R.,** Self-potential prospecting in the deep oceans, *Geology,* 3, 541, 1975.
115. **Nebrija, E. L., Young, C. T., Meyer, R. P., and Moore, J. R.,** Electrical prospecting for cooper veins in shallow water, Offsh. Tech. Conf., Houston, TX, OTC paper #2454, 319, 1976.
116. **Young, P. D. and Cox, C. S.,** The electrical conductivity of the crust near the East Pacific Rise inferred from electromagnetic measurements: correlation with seawater content of the crust, *Eos Trans. AGU,* 61, 993, 1980.
117. **Young, P. D. and Cox, C. S.,** Electromagnetic source active sounding near the East Pacific Rise, *Geophys. Res. Lett.,* 8, 1043, 1981.
118. **Becker, K., Von Herzen, R. P., Francis, T. J., Anderson, R. N., Honnorez, J., Adamson, A. C., Alt, J. C., Emmermann, R., Kempton, P. D., Kinoshita, H., Laverne, C., Mottl, M. J., and Newmark, R. L.,** *In situ* electrical resistivity and bulk porosity of the ocean crust Costa Rica Rift, *Nature,* 300, 594, 1982.
119. **Edwards, R. N., Law, L. K., Wolfgram, P. A., Nobes, D. C., Bone, M. N., Trigg, D. F. and Delaurier, J. M.,** First results of the MOSES experiment: sea sediment conductivity and thickness determination, Bute Inlet, British Columbia, by magnetometric offshore electrical sounding, *Geophysics,* 50, 153, 1985.
120. **Becker, K.,** Large scale resistivity and bulk porosity of the oceanic crust, Hole 504B, Costa Rica Rift, *Init. Rept. Deep Sea Drill. Proj.,* 83, 419, 1985.
121. **Wolfgram, P. A., Edwards, R. N., Law, L. K., and Bone, M. N.,** Polymetallic sulfide exploration on the deep sea floor: the feasibility of the MINI-MOSES technique, *Geophysics,* 51, 1808, 1986.
122. **Edwards, R. N. and Chave, A.,** A transient electric dipole-dipole method for mapping the conductivity of the sea floor, *Geophysics,* 51, 984, 1986.
123. **Cheesman, S. J., Edwards, R. N., and Chave, A. D.,** On the theory of sea-floor conductivity mapping using transient electromagnetic systems, *Geophysics,* 52, 204, 1987.
124. **Combs, J. and Hadley, D. M.,** Microearthquake investigation of the Mesa geothermal anomaly, Imperial Valley, California, *Geophysics,* 42, 17, 1977.
125. **Jarzabek, D. and Combs, J.,** Microearthquake survey of the Dunes KGRA, Imperial Valley, Southern California, *Geol. Soc. Am.,* 8(Abstr.), 939, 1976.
126. **Quillan, R. and Combs, J.,** Microearthquake survey of the Radium springs KGRA south central New Mexico, *Geol. Soc. Am.,* 8(Abstr.), 1055, 1976.
127. **Johnson, D. M. and Combs, J.,** Microearthquake survey of the Kilbourne Hole KGRA south central New Mexico, *Geol. Soc. Am.,* 8(Abstr.), 942, 1976.
128. **Ward, P. L., Palmason, G., and Drake, C.,** Microearthquake survey and the Mid-Atlantic Ridge in Iceland, *J. Geophys. Res.,* 74, 665, 1969.
129. **Ward, P. L. and Bjornsson, S.,** Microearthquakes swarms and the geothermal areas of Iceland, *J. Geophys. Res.,* 76, 3953, 1971.
130. **Klein, F. W., Einarsson, P., and Wyss, M.,** Microearthquakes on the Mid-Atlantic plate boundary on the Reykjanes Peninsula in Iceland, *J. Geophys. Res.,* 78, 5084, 1973.
131. **Rinehart, J. S.,** Fluctuations in geyser activity caused by variations in earth tidal forces, barometric pressure, and tectonic stress, *J. Geophys. Res.,* 77, 342, 1972.
132. **Trimble, A. B. and Smith, R. B.,** Seismicity and contemporary tectonics of the Hebegen Lake-Yellowstone Park region, *J. Geophys. Res.,* 80, 733, 1975.
133. **Smith, R. B., Shuey, R. T., Pelton, J. R., and Bailey, J. P.,** Yellowstone hot spot: contemporary tectonics and crustal properties from earthquakes and aeromagnetic data, *J. Geophys. Res.,* 82, 3665, 1977.
134. **Oppenheimer, D. H.,** Extensional tectonics at the Geysers Geothermal area, California, *J. Geophys. Res.,* 91, 11463, 1986.
135. **Francis, T. J.,** The detailed seismicity of mid-oceanic ridges, *Earth Planet. Sci. Lett.,* 4, 39, 1968.

136. **Sykes, L.,** Focal mechanism solutions for earthquakes along the world rift system, *Bull. Seismol. Soc. Am.*, 60, 1749, 1970.
137. **Isacks, B., Oliver, J., and Sykes, L.,** Seismology and the new global tectonics, *J. Geophys. Res.*, 73, 5855, 1968.
138. **Huang, P. Y., Solomon, S. C., Bergman, E. A., and Nabelek, J. L.,** Focal depths and mechanisms of Mid-Atlantic Ridge earthquakes from body waveform inversion, *J. Geophys. Res.*, 91, 579, 1986.
139. **Macdonald, K. C. and Mudie, J. D.,** Microearthquakes on the Galapagos spreading center and the seismicity of fast spreading ridges, *Geophys. J. R. Astron. Soc.*, 36, 245, 1974.
140. **Reidesel, M., Orcutt, J. A., Macdonald, K. C., and McClain, J. S.,** Microearthquakes in the Black Smoker Hydrothermal Field, East Pacific Rise at 21°N, *J. Geophys. Res.*, 87, 10613, 1982.
141. **Kong, L., Solomon, S. C., and Purdy, G. M.,** Microearthquakes near the TAG hydrothermal field, Mid-Atlantic Ridge, 26°N, *Eos Trans. AGU*, 67, 1021, 1986.
142. **Bibee, D. and Jacobson, R.,** Acoustic noise measurements on Axial seamount, Juan de Fuca Ridge, *Geophys. Res. Lett.*, 13, 957, 1986.
143. **Jacobson, R. S., Bibee, L. D., Embley, R. W., and Hammond, S. R.,** A microseismicity survey of Axial seamount, Juan de Fuca Ridge, *Bull. Seismol. Soc. Am.*, 77, 160, 1987.
144. **Little, S. A., Purdy, G. M., and Stolzenbach, K. D.,** Acoustic monitoring of hydrothermal vent fields, *Eos Trans. AGU*, 67, 1232, 1986.
145. **Laughton, A. S.,** The first decade of GLORIA, *J. Geophys. Res.*, 86, 11511, 1981.
146. **Spiess, F. N. and Lonsdale, P.,** Deep tow rise crest exploration techniques, *Mar. Technol. Soc. J.*, 16, 67, 1982.
147. **Simoneit, B. and Lonsdale, P.,** Hydrothermal petroleum mineralised mounds at the seabed at Guaymas Basin, *Nature*, 295, 198, 1982.
148. **Blackinton, J. G., Hussong, D. M., and Kosalos, J. G.,** First results from a combination side-scan sonar and seafloor mapping system (SeaMARC II), *Proc. Offsh. Tech. Conf.*, 307, 1983.
149. **Hussong, D. M. and Fryer, P.,** Back-Arc seamounts and the SeaMARC II seafloor mapping system, *Eos Trans. AGU*, 64, 627, 1983.
150. **Kosalos, J. G.,** Ocean bottom imaging, *Proc. Offsh. Tech. Conf.*, 2, 65, 1984.
151. **Davis, E. E., Currie, R. G., Riddihough, R. P., Ryan, W. B., Kastens, K., Hussong, D. M., Hammond, S. R., and Malahoff, A.,** Geological mapping of the northern Juan de Fuca and Explorer Ridges using SeaMARC I, SeaMARC II, and Seabeam acoustic mapping, *Eos Trans. AGU*, 65, 1110, 1984.
152. **Villinger, H. and Davis, E. E.,** Heat-flow and bottom water temperature measurements from the rift valley of the northern Juan de Fuca Ridge, *Eos Trans. AGU*, 65, 1111, 1984.
153. **Franklin, J.,** personal communication, 1987.
154. **Currie, R. G., Davis, E. E., Riddihough, R. P., and Sawyer, B. S.,** Juan de Fuca Ridge Atlas: preliminary Seabeam bathymetry, *Geol. Surv. Can. Open File*, 1143, 1985.
155. **Allis, R. G. and Hunt, T. M.,** Analysis of exploitation induced gravity changes at Wairakei geothermal field, *Geophysics*, 51, 1647, 1986.
156. **Jachens, R. C. and Roberts, C. W.,** Temporal and areal gravity investigations at Long Valley Caldera, California, *J. Geophys. Res.*, 90, 11210, 1985.
157. **Luyendyk, B. P.,** On bottom gravity profile across the East Pacific Rise at 21° north, *Geophysics*, 49, 2166, 1984.
158. **Styrt, M. M., Brackman, A. J., Holland, H. D., Clark, B. C., Pisutha-Arnold, V., Eldridge, C. S., and Ohmoto, H.,** The mineralogy and the isotopic composition of sulfur in hydrothermal sulfide/sulfate deposits on the East Pacific Rise, 21°N latitude, *Earth Planet. Sci. Lett.*, 53, 382, 1981.
159. **Haymon, R. M. and Kastner, M.,** Hot spring deposits on the East Pacific Rise at 21°N: preliminary description of mineralogy and genesis, *Earth Planet. Sci. Lett.*, 53, 363, 1981.
160. **Hekinian, R., Francheteau, F., Renard, V., Ballard, R. D., Chaukroune, P., Cheminee, J. L., Albarede, F., Minster, J. F., Charlou, J. L., Marty, J. C., and Boulegue, J.,** Intense hydrothermal activity at the rise axis of the EPR near 13°N: submersible witnesses the growth of sulfide chimney, *Mar. Geophys. Res.*, 6, 1, 1983.
161. **Alt, J., Lonsdale, P., Haymon, R., and Muehlenbachs, K.,** Hydrothermal sulfide and oxide deposits on seamounts near 21°N, East Pacific Rise, *Geol. Soc. Am. Bull.*, submitted.
162. **McConachy, T. F., Ballard, R. D., Mottl, M. J., and von Herzen, R. P.,** The geological form and setting of a hydrothermal vent field at 10° 56′N, East Pacific Rise: a detailed study using ANGUS and ALVIN, *Geology*, 14(4), 295, 1986.
163. **Tunnicliffe, V., Botros, M., DeBurgh, M. E., Dinet, A., Johnson, H. P., Juniper, S. K., and McDuff, R. E.,** Hydrothermal vents of Explorer Ridge, northeast Pacific, *Deep-Sea Res.*, 33(3A), 401, 1986.
164. **Chase, R. L., Delaney, J. R., Karsten, J. L., Johnson, H. P., Juniper, S. K., Lupton, J. E., Scott, S. D., Tunnicliffe, V., Hammond, S. R., and McDuff, R. E.,** Hydrothermal vents on an Axis Seamount of the Juan de Fuca Ridge, *Nature*, 313, 212, 1985.
165. **Normark, L., Lupton, J. E., Murray, J. W., Koski, R. A., Clague, D. A., Morton, J. L., Delaney, J. R., and Johnson, H. P.,** Polymetallic sulfide deposits and water column tracers of active hydrothermal vents on the southern Juan de Fuca, *Mar. Technol. Soc. J.*, 16(3), 46, 1982.
166. **Koski, R. A., Clague, D. A., and Oudin, E.,** Mineralogy and chemistry of massive sulfide deposits from the Juan de Fuca, *Geol. Soc. Am. Bull.*, 95, 930, 1984.
167. **Koski, R. A., Haymon, R. M., and Abrams, M.,** Ridge-crest and offridge hydrothermal-discharge zones mapped beneath massive sulfide deposits in the Samail Ophiolite, Northern Oman, *Eos Trans. AGU*, 68, 1545, 1987.
168. **Constantinou, G.,** Metallogenesis associated with the Troodos ophiolite, in Ophiolites, Proc. Int. Ophiolite Symp., Cyprus, Ministry of Agriculture and Natural Resources, Nicosia, Cyprus, 1979.
169. **Adamides, N. G.,** The form and environment of formation of the Kalavasos ore deposits, Cyprus, in Ophiolites, Proc. Int. Ophiolite Symp., Cyprus, Ministry of Agriculture and Natural Resources, Nicosia, Cyprus, 1979.
170. **Goldfarb, M. S., Converse, D. R., Holland, H. D., and Edmond, J. M.,** The genesis of hot spring deposits on the East Pacific Rise, 21°N, in *Econ. Geological Monograph 5*, Ohmoto, H. and Skinner, B. J., Eds., 1983, 184.
171. **Hekinian, R. and Fouquet, Y.,** Volcanism and metallogenesis of axial and off-axial structures on the East Pacific Rise near 13° N, *Econ. Geol.*, 80, 221, 1985.
172. **Johnson, H. P.,** personal observations, 1984.
173. **Tunnicliffe, V. and Juniper, M. de Burgh,** The hydrothermal community on Axial seamount, Juan de Fuca Ridge, in The Hydrothermal Vents of the Eastern Pacific: An Overview, Jones, M., Ed., *Bull. Biol. Soc. Wash.*, 6, 453, 1985.
174. **Johnson, H. P. and Tunnicliffe, V.,** Time-series measurements of hydrothermal activity on the northern Juan de Fuca Ridge, *Geophys. Res. Lett.*, 12, 685, 1985.
175. **Johnson, H. P. and Tunnicliffe, V.,** Time-lapse camera measurements of a high temperature hydrothermal system on axial seamount, Juan de Fuca Ridge, *Eos Trans. AGU*, 67, 1283, 1986.
176. **Morton, J. L., Holmes, M. L., and Koski, R. A.,** Volcanism and massive sulphide formation at a sedimented spreading center, Escanaba Trough, Gorda ridge, Northeast Pacific Ocean, *Geophys. Res. Lett.*, 14, 769, 1987.
177. **Franklin, J. M., Goodfellow, W. D., Blaise, B., Anglin, C. D., Harvey-Kelly, F. L., Macdonald, R., and Kappel, E.,** Geological map and distribution of sulfide deposits in Middle Valley, Northern Juan de Fuca Ridge, *Eos Trans. AGU*, 68, 1545, 1987.

178. **Delaney, J. R., Spiess, F. N., Solomon, S. C., Hessler, R., Karsten, J. L., Baross, J. A., Holcomb, R. T., Norton, D., McDuff, R. E., Sayles, F., Whitehead, J., Abbott, D., and Olsen, L.,** Scientific rationale for establishing long-term ocean bottom observatory/laboratory systems, in *Marine Minerals,* Teleki, P. G., Ed., Reidel Publishing, 1987, 389.